Exploring Environmental Modifiers of LRRK2-Associated Parkinson's Disease Penetrance through Exposomics and Metagenomics of Household Dust

Begoña Talavera Andújar[1*], Sandro L. Pereira[1], Susheel Bhanu Busi[1,2], Tatiana Usnich[3], Max Borsche[3,4], Sibel Ertan[5], Peter Bauer[6], Arndt Rolfs[6], Soraya Hezzaz[1], Jenny Ghelfi[1], Norbert Brüggemann[3,4], Paul Antony[1], Paul Wilmes[1,7°], Christine Klein[3°], Anne Grünewald[1°], Emma L. Schymanski[1*°]

[1] Luxembourg Centre for Systems Biomedicine (LCSB), University of Luxembourg, L-4367 Belvaux, Luxembourg

[2] UK Centre for Ecology and Hydrology, Wallingford, Oxfordshire, United Kingdom

[3] Institute of Neurogenetics, University of Lübeck, Lübeck, Germany

[4] Department of Neurology, University of Lübeck, Lübeck, Germany

[5] School of Medicine, Department of Neurology, Koc University, Istanbul, Turkey

[6] CENTOGENE GmbH, Rostock, Germany

[7] Department of Life Sciences and Medicine, Faculty of Science, Technology and Medicine, University of Luxembourg, L-4362 Esch-sur-Alzette, Luxembourg

°Shared senior authors: PW, CK, AG, ELS

*Corresponding authors: BTA: begona.talavera@uni.lu and ELS: emma.schymanski@uni.lu

ORCIDS: BTA, 0000-0002-3430-9255; SLP, 0000-0001-9498-3965; SBB, 0000-0001-7559-3400; TU, 0000-0001-7335-8888; MB, 0000-0002-9651-5986; SE, 0000-0003-1339-243X; PB, 0000-0001-9414-4555; SH, 0009-0009-5984-2767; JG, 0009-0000-4551-6033; NB, 0000-0001-5969-6899; PA, 0000-0002-0450-9301; PW, 0000-0002-6478-2924; CK, 0000-0003-2102-3431; AG, 0000-0002-4179-2994; ELS, 0000-0001-6868-8145

Keywords: Indoor environment, exposomics, metagenomics, Parkinson's disease, *Leucine-rich repeat kinase 2 (LRRK2),* bisphenol S

Highlights

- Exposomics of household dust revealed several significant chemicals of interest
- Chemical replacements Bisphenol S (BPS) and PFBuS may modify *LRRK2* penetrance
- BPS negatively impacted mitochondria in dopaminergic neuron-enriched cultures
- Benzothiazoles may be degraded by *Pseudomonas* spp. identified by metagenomics
- Lipid species were altered in the serum of the PD+/LRRK2+ individuals *vs* controls

Graphical Abstract

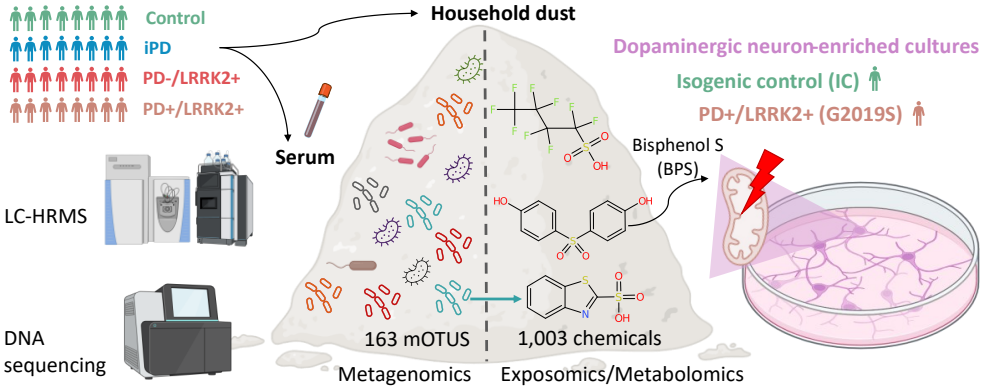

Abstract

Pathogenic variants in the *Leucine-rich repeat kinase 2* (*LRRK2*) gene are a primary monogenic cause of Parkinson's disease (PD). However, the likelihood of developing PD with inherited *LRRK2* pathogenic variants differs (a phenomenon known as "reduced penetrance"), with factors including age and geographic region, highlighting a potential role for lifestyle and environmental factors in disease onset. To investigate this, household dust samples from four different groups of individuals were analyzed using metabolomics/exposomics and metagenomics approaches: PD+/LRRK2+ (PD patients with pathogenic *LRRK2* variants; n=11), PD-/LRRK2+ (individuals with pathogenic *LRRK2* variants but without PD diagnosis; n=8), iPD (PD of unknown cause; n=11), and a matched, healthy control group (n=11). The dust was complemented with metabolomics and lipidomics of matched serum samples, where available. A total of 1,003 chemicals and 163 metagenomic operational taxonomic units (mOTUs) were identified in the dust samples, of which ninety chemicals and ten mOTUs were statistically significant. Reduced levels of 2-benzothiazolesulfonic acid ($BThSO_3$) were found in the PD-/LRRK2+ group compared to the PD+/LRRK2+. A negative and statistically significant association was observed between $BThSO_3$ and *Pseudomonas* spp. (detected via metagenomics), which are known for degrading benzothiazoles. Among the significant chemicals tentatively identified in dust, two are hazardous chemical replacements: Bisphenol S (BPS), and perfluorobutane sulfonic acid (PFBuS). Furthermore, various lipids were found altered in serum including different lysophosphatidylethanolamines (LPEs), and lysophosphatidylcholines (LPCs), some with higher levels in the PD+/LRRK2+ group compared to the control group. A cellular study on isogenic neurons generated from a PD+/LRRK2+ patient demonstrated that BPS negatively impacts mitochondrial function, which is implicated in PD pathogenesis. This pilot study demonstrates how non-target metabolomics/exposomics analysis of indoor dust samples complemented with metagenomics can prioritize relevant chemicals that may be potential modifiers of *LRRK2* penetrance.

1. Introduction

Parkinson's disease (PD) is a neurodegenerative disorder, affecting 1.8% of individuals over the age of 80 years globally, with an increasing prevalence due to the progressive aging of the population [1]. PD is characterized by the abnormal accumulation of misfolded alpha-synuclein (α-syn) inside neurons, leading to the formation of Lewy Bodies, which promote neuroinflammation and the irreversible degeneration of dopaminergic neurons in the *substantia nigra pars compacta* and other brain regions [2], [3], [4], [5]. The clinical hallmarks of PD are tremor, bradykinesia, rigidity, and later in the disease, postural instability [2]. However, these typical motor features do not become evident until 60-80% of dopaminergic neurons are lost, such that other indicators are needed for earlier diagnosis [6]. Non-motor symptoms related to PD, such as constipation and REM-sleep behavior disorder (RBD), can occur decades before the onset of the classical motor symptoms but often go unrecognized [2], [5], [6], [7]. Since not all PD patients have Lewy bodies or positive α-syn readings [8], [9], recently, a biological classification of PD has been proposed for research purposes, which considers the presence or absence of α-syn pathology, features of neurodegeneration, and genetic contributions [10].

Although the exact cause of most of patients with PD remains unknown, recent studies suggest that a combination of genetic and environmental risk factors may play a key role in the development of the disease [2], [6], [11]. Typically, monogenic PD comprises five dominantly inherited forms (*SNCA*, *LRRK2*, *VPS35, RAB32* and *CHCHD2*) and three recessively inherited forms (*PRKN*, *PINK1*, and *PARK7*) [10], [11]. Mitochondrial dysfunction may occur already in the early stages of PD pathogenesis and plays a crucial role in both sporadic and familial forms of the disease [12], [13]. Gene variants of *Leucine-rich repeat kinase 2* (*LRRK2*) are the most common monogenic cause of PD, accounting for 1-2% of all cases [14], [15], [16], [17]. Most of the *LRRK2* pathogenic variants result in increased kinase activity of the LRRK2 protein, leading to mitochondrial dysfunction and promoting inflammatory responses that may result in chronic neuroinflammation and gut inflammation [2], [15]. In addition to PD, LRRK2 has been linked to inflammatory diseases including Crohn's Disease, leprosy and tuberculosis [2], [18]. While the p.G2019S pathogenic variant of *LRRK2* is the best known and most common, not all carriers of this variant will develop PD, a phenomenon termed "reduced penetrance" [2], [15], [19], [20]. Importantly, the penetrance is age-dependent and differs across geographic regions. For example, in Tunisia, 61% of *LRRK2* p.G2019S carriers developed PD by the age of 60 years, and 86% by the age of 70. In contrast, in Norway, only 20% of carriers developed the disease by age 60, and 43% by age 70 [19], [21]. This suggests that factors beyond genes, such as lifestyle or environment, may play a crucial role in triggering the onset of the disease [2]. Various environmental factors have been previously associated with an increased risk of PD, including the exposure to metals (e.g., Cu, Fe and Zn) and pesticides (e.g., rotenone and paraquat) [22]. In contrast, smoking, caffeine consumption, and the use of anti-inflammatory drugs have been linked with a reduced PD risk [22], [23]. The

LRRK2/Luebeck International Parkinson's Disease Study (LIPAD) cohort is one of the largest multinational cohorts of genetic PD, focused on LRRK2-associated PD and healthy *LRRK2* pathogenic variant carriers aiming to identify modifiers of *LRRK2* penetrance [19]. This study includes the household dust from selected LIPAD cohort participants to determine whether this can potentially reveal potential chemical exposures and taxa of interest that may influence *LRRK2* penetrance.

In urban environments, humans spend about 90% of their time indoors [24], exposing themselves to a wide range of chemicals and microbes that may enter the body via ingestion, inhalation or dermal contact [25], and could have an impact on health. Dust acts as a repository of multiple compounds that are present or transported indoors and thus could be an indicator of the "human exposome" [26]. Estimates of the number of chemicals in household use range between 30,000 and 70,000 [27]. Nevertheless, most studies investigating dust so far have involved targeted analyses i.e., limited only to dozens of chemicals [15], [26], while house dust can be contaminated with a broad range of chemicals including pesticides, personal care products, and plasticizers, which can only be explored in greater detail using a non-target approach [26], [28]. PubChem, which contains 118 million chemicals as of July 2024, is one source of such information [29], but is too large for efficient cheminformatics workflows. Instead, the PubChemLite for Exposomics collection leverages the comprehensive knowledgebase within PubChem to form a relevant subset for exposomics studies, compiled from ten different categories in the PubChem Compound Table of Contents (TOC) Classification Browser [30], comprising ~400,000 chemicals [31], [32]. Other environmentally relevant information sources include the NORMAN Suspect List Exchange (NORMAN-SLE) [33], which is a collection of more than 100 lists of chemicals covering a wide range of chemical classes contributed by the environmental community and compiled by the NORMAN network [34], [35]. NORMAN-SLE lists are given a "S" number and code and include collections such as cosmetics (e.g., S13 EUCOSMETICS [36]), chemicals registered for use in Europe exceeding one tonne per year (S32 REACH2017 [37]), and neurotoxicants (e.g., S37 LITMINEDNEURO [38]). In 2016, the NORMAN network organized a collaborative non-target trial on household dust, with close to 2,350 compounds identified or tentatively identified in those dust samples [26]. The results are also available in the NORMAN-SLE as suspect list (S35 INDOORCT16) [26], [39]. Both gas chromatography-mass spectrometry (GC-MS), and liquid chromatography-mass spectrometry (LC-MS) were used, with only 5% of the detected compounds overlapping between these two techniques. While LC-MS allowed the detection of glycols, pharmaceuticals, pesticides, and biogenic compounds in the samples, GC-MS detected more non-polar compounds, including hydrocarbons and chlorinated paraffins [26].

Household dust also acts as the main reservoir of microbial taxa in the domestic environment, since it includes particulate matter from soil, plants, human and animal skin. The household dust microbiome influences the host microbiome [24], with some studies investigating the potential effects of dust-borne

microbial taxa on allergy, asthma, immune system, and gut microbiome [24], [40], [41]. One of the challenges of metagenomic studies of dust samples is the high diversity of indoor microorganisms, with an overall microbial diversity on Earth estimated to be approximately one trillion organisms [42], and between 500 and 1,000 different species reported in household dust [43]. A study examining paired samples of dust and feces revealed significant co-occurrences of *Actinobacteria, Bacilli, Clostridia* and *Gamma proteobacteria* in both samples [44]. Another study indicated a potential link between household dust exposure and sphingolipid metabolism impairment associated with allergic processes [45]. Furthermore, the dust microbiome may be involved in the biotransformation of chemicals analogous to what is seen in other environments [46]. Household dust also contains multiple endocrine-disrupting chemicals impacting human physiology, leading to triglyceride accumulation in in vitro models (pre-adipocyte mouse cells) [47]. Alterations in metabolism due to environmental exposures, including household dust, may be partially attributed to the effect of dust modulating the host microbiome, as previously proposed [44]. Household dust is a diverse mixture of artificial and natural particles along with biological entities such as bacteria, molds and pollen, as well as ash, soot, skin particles, and residues from building and consumer products [48]. Consequently, the analysis of household dust is of great interest to investigate the human exposome, offering valuable insights into the individuals' environmental exposures.

As part of the LIPAD study [19], this work aims to identify potential environmental modifiers of the penetrance of *LRRK2* pathogenic variants through the analysis of household dust of four groups of participants: PD+/LRRK2+ (PD individuals with pathogenic *LRRK2* variants), PD-/LRRK2+ (individuals with pathogenic *LRRK2* variants but without PD diagnosis), iPD (PD of unknown cause), and a matched control group (individuals without pathogenic variants and without PD diagnosis), through different metabolomics/exposomics and metagenomics approaches. This was complemented with non-target metabolomics on paired serum samples, where available, to investigate potential metabolomic differences between groups that could be attributed to environmental exposures. Additionally, since alterations in bile acids (BAs) have been previously noted in PD [49], [50], [51], a target study of BAs in serum was performed. Finally, a cell study in isogenic neurons generated from a PD+/LRRK2+ patient was conducted to investigate the potential neurotoxic effects of a chemical found in the household dust, using various readouts related to mitochondrial function. To our knowledge, this is the first study investigating the environmental influences of *LRRK2* penetrance through the molecular analysis of household dust.

2. Material and methods

2.1. Sample collection

Samples from four different groups of individuals (Control, iPD, PD-/LRRK2+, PD+/LRRK2+, explained above) were collected in Germany (36) and Turkey (4), with details provided in **Table 1**. Additional information has already been published [19]. Participants with different *LRRK2* variants were included in this study. In the PD+/LRRK2+ group, seven participants carried the p.G2019S variant, two had the p.N1437S variant, and one each had the p.R1441H and p.I2020T variants. In the PD-/LRRK2+ group, six individuals carried the p.G2019S variant, while one each had the p.R1441C and p.S901L variants. Importantly, carriers of pathogenic and likely pathogenic variants in 68 PD-linked genes were excluded in the iPD and control groups, as specified in the ROPAD protocol [16], [52].

Table 1. *Demographic characteristics of the studied groups (mean ± standard deviation). (a) ANOVA single factor was applied to calculate the p-value of the age across groups, while Chi-square p-value was computed for the categorical variable (sex).*

Sample	Details	Control	iPD	PD-/LRRK2+	PD+/LRRK2+	p-value[(a)]
Dust	n	11	11	8	11	
	Age	60.54± 11.15	62.45± 7.88	50.75± 10.40	61.73± 8.33	0.0487
	Sex (f/m)	6/5	6/5	7/1	6/5	0.4012
Serum	n	8	3	8	5	
	Age	60.40± 9.27	65.00± 6.00	50.75± 10.40	58.20± 8.38	0.6864
	Sex (f/m)	5/3	3/0	7/1	1/4	0.0455

A total of forty-one dust samples were collected from vacuum cleaner bags provided by the participants and stored at room temperature until analysis. In addition, twenty-four matched serum samples were collected (**Table 1**) and stored at –80 °C until the analysis. **Figure 1** shows the number of samples per group, and the analyses performed (described further in the following sections).

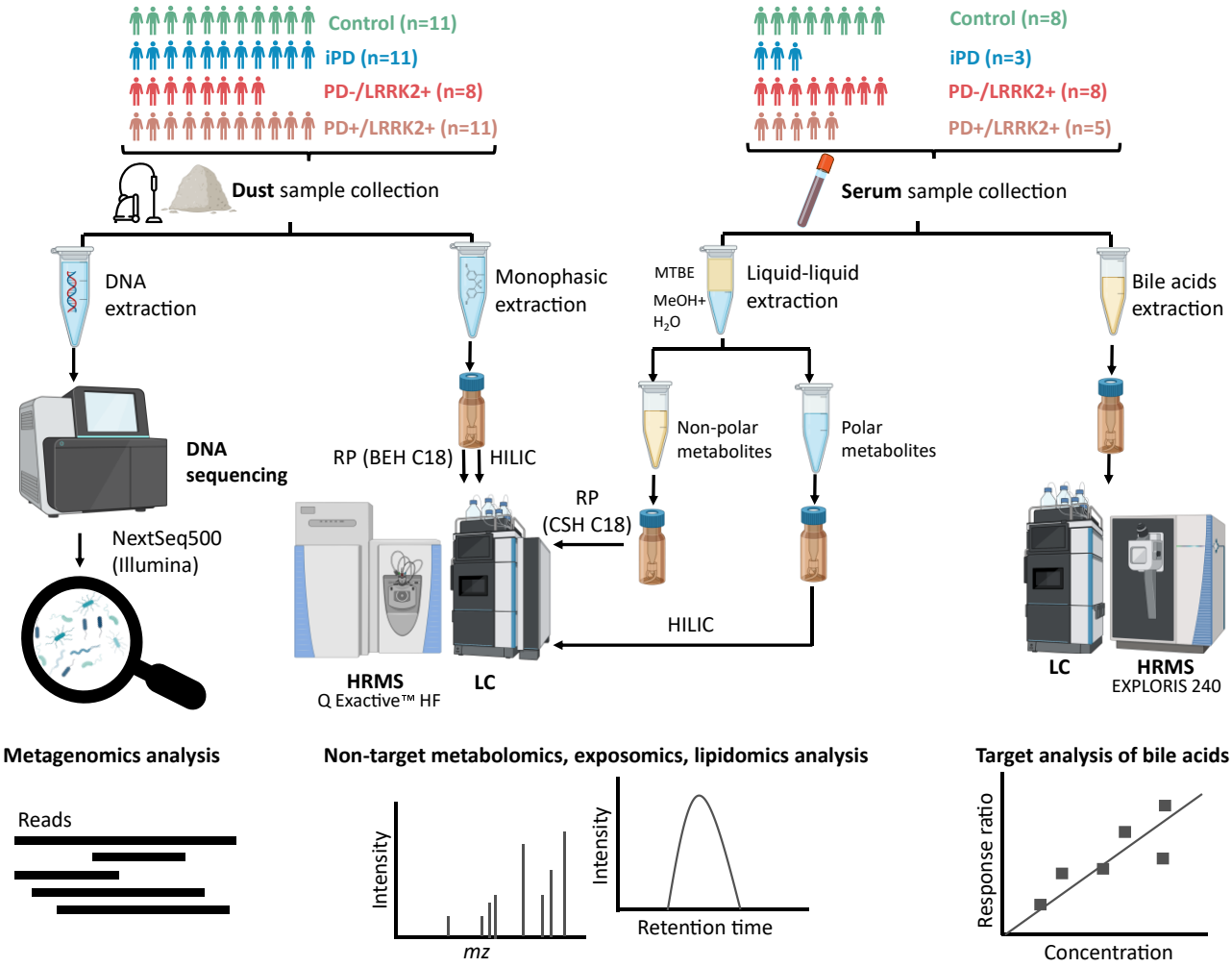

154

155 ***Figure 1.*** *Scheme showing the four groups under study, type of samples analyzed (dust and serum), as well*
156 *as the different analyses performed in each of them. Note that all the serum samples were matched with*
157 *the dust.*

158

159 ## 2.2. Sample preparation

160 ### 2.2.1. Dust

161 The sample extraction protocol for metabolomics/exposomics was adapted from Moschet *et al.* [28]
162 and Dubocq *et al.* [53]. Briefly, 50 mg of each dust sample was extracted using acetonitrile (ACN):
163 methanol (MeOH) (1:1, v/v). The extract was evaporated (Labconco CentriVap, -4 °C, 24-48 h),
164 reconstituted using 0.1 % formic acid (FA) in MilliQ water and MeOH (90:10, v/v), and filtered
165 (Phenex-RC 4 mm syringe filter, 0.2 μm). Ten internal standards were used to check the instrument
166 performance (see **Table S1**). Extraction blanks and quality control (QC) samples (**Figure S1**) were

prepared following the guidelines from Broadhurst *et al.* [54]. A standard mix of 170 polar compounds (50 μM) was used to serve as reference standards later (see **Table S2** for full listing). Further details are given in the Supplementary Material (SM), section **S1.1.1**.

For the metagenomic analyses, 100 mg of each dust sample were aliquoted, and DNA was extracted using the DNeasy PowerLyzer PowerSoil Kit (Qiagen, 12855-50). Tests were performed at three input amounts (50 mg, 100 mg, and 150 mg), whereby 100 mg of material yielded the best output in terms of DNA concentrations and quality, see **S1.1.1** (**Figure S2-S3**) for details. The manufacturer's protocol was followed [55], with the exception that DNA extracts were eluted in 40 μL of sterile DNA-free PCR-grade water instead of 100 μL of Solution C6.

2.2.2. Serum

The protocol for the non-target LC-HRMS analysis was adapted from Cajka *et al.* [56] and Lange *et al.* [57], detailed in full in **S1.1.2** and shown in **Figure S4**. Briefly, serum samples were thawed on ice and extracted via liquid-liquid extraction (LLE) with cold MeOH containing 14 SPLASH® LIPIDOMIX® mass spectrometry standards (listed in **Table S3**, chromatograms shown in **Figure S5-S6**), methyl tert-butyl ether (MTBE), containing cholesteryl ester 22:1 (CE22:1), and MilliQ water. The QC, extraction blank samples, and the standard polar mix of 170 compounds (**Table S2**) were as described for the dust samples.

For the targeted BA analysis, 50 μL of each serum sample was extracted with MilliQ water (containing four IS) and cold MeOH. The IS were cholic-D4 acid (CA-D4), deoxycholic-D4 acid (DCA-D4), lithocholic-D4 (LCA-D4), and glycocholic-D4 acid (GCA-D4). A mixture of fourteen targeted BAs (10 μg/mL) was prepared (listed in **Table S4**). This standard solution was further diluted step by step to build the calibration curve. Further details are given in **S1.1.2**.

2.3. Instrumental analysis

2.3.1. Metabolomics/Exposomics/Lipidomics

Non-target analysis of dust and serum was performed on a Thermo Scientific Accela LC system coupled to a Q Exactive™ HF (Thermo Scientific) mass spectrometer using electrospray ionization (ESI) in both positive (+) and negative (-) ionization modes. Dust samples were analyzed using an Acquity BEH C_{18} reversed phase (RP) column (150 × 2.1 mm; 1.7 μm), and a SeQuant® ZIC-pHILIC 5 μm polymer (HILIC) column (150 × 2.1 mm), each with the respective guard column. The HILIC method was also employed to analyze the polar extracts of the serum samples. The HRMS was operated in full scan profile mode with a scan range of 60-900 *m/z*. Complete details of the RP and HILIC LC-HRMS methods are given in Talavera Andújar *et al.* [4].

The non-polar extracts of the serum samples were analyzed (lipidomics) with an RP method adapted from a Cajka *et al.* [56], using an Acquity UPLC CSH C_{18} RP column (100 × 2.1 mm; 1.7 μm) coupled to a guard column (130Å, 1.7 μm, 2.1 mm X 5 mm). Full details are given in **S1.2.1**.

2.3.2. Target Analysis of BAs

The target analysis of BAs (**Table S4**) was performed on a LC system coupled to a Thermo Orbitrap Exploris 240. The HRMS was operated in negative ionization mode (full scan mode) with a scan range of 100-620 m/z, with the same column as for the lipidomics analysis. Full details are given in **S1.2.2**.

2.3.3. Metagenomic analyses

DNA was quantified using Qubit fluorometer and Quant-iT dsDNA HS Assay kits to obtain accurate concentration values. A Nanodrop instrument was then employed to determine DNA quality through the 260/280 and 260/230 ratios (**Table S5**). DNA libraries were prepared after PCR amplification, taking the same starting DNA from each sample. 50 ng of DNA were used for metagenomic library preparation using the xGen DNA library preparation kit (Cat. no. 10009822, Integrated DNA Technologies) using xGen UDI-UMI adapters (Cat. no. 10005903). The genomic DNA was enzymatically fragmented for 10 min and DNA libraries were prepared with PCR amplification. The average insert size of libraries was 400 bp. Prepared libraries were quantified using Qubit (DNA HS kit, Thermo) and quality checked with DNA HS kit on Bioanalyzer 2100 (Agilent). Sequencing was performed at the LCSB Genomics Platform (RRID: SCR_021931) on NextSeq2000 (Illumina) instrument using 2x150 bp read length.

2.4. Data Analysis

2.4.1. Metabolomics/Exposomics/Lipidomics

For the dust and serum (polar extracts), raw files (".raw") were converted to ".mzML" format using ProteoWizard MSConverter (Version 3.0.20331.3768aa6e9 64-bit) [58]. The converted files were analyzed with the open software patRoon (version 2.1.0) [59], [60], using the non-target and suspect screening options. This was complemented with MS-DIAL (version 4.9.221218) [61] using version 17 of the MSP libraries; the MS-DIAL input parameters are given in **Table S6**. Further details are given in **S1.3.1** and **Figure S7;** the code for patRoon is available on GitLab [62].

For the lipid analysis in serum, the LC-HRMS raw data files were processed in MS-DIAL (parameters given in **Table S7**) using the *in silico* LipidBlast [63] library. To complement the MS-DIAL lipid annotations, which are similarity-based, LipidMatch [64], a rule based software, was employed (see **Figure S8**). The annotations from MS-DIAL and LipidMatch were combined; LipidMatch annotations were selected in case of duplicates.

Among all features identified by non-target and suspect screening approaches in dust and serum, only those with MS/MS information and MS/MS match values were considered for further analysis and chemical annotation. R (version 4.1.2) via RStudio (version 2022.02.3) was used to filter the samples. Features with a relative standard deviation (RSD) > 50 % in the QC-pooled samples were discarded. Since different cheminformatic approaches and software were employed to analyze the non-target and suspect screening LC-HRMS data, four different types of criteria were used to annotate confidence levels to the features (**Table S8**). Note that only high confidence features, Level 1 to Level 3 (matching various criteria shown in **Table S8**), were considered in this study to ensure the quality of the biological interpretation. Features were annotated as Level 1 when the match between the chemical standard (**Table S2**) and tentative candidate (in the dust or serum) yielded a SpectrumSimilarity score ≥ 0.7 and the retention time (RT) shift was <1 min. *OrgMassSpecR* [65], [66] was used to calculate spectral similarity. Xcalibur Qual Browser (version 4.1.31.9) was used to check the RT and to extract the MS/MS information. The annotated chemicals were classified using the MetOrigin web server [67] and the PubChem Classification Browser [29], using both the PubChem Compound TOC [30] and the NORMAN-SLE [68] browsers. Chemical structures generated using CDK Depict [69].

For the statistical analysis, peak intensity tables were uploaded to MetaboAnalyst 6.0 (web interface) [70], normalized by sum, $\log_{10}$ transformed and Pareto-scaled. Principal Component Analysis (PCA) was performed using MetaboAnalyst 6.0 while Analysis of Variance (ANOVA) with Tukey's honestly significant difference (HSD) post hoc test was computed in R (version 4.1.2). A p-value < 0.05 was considered as statistically significant in this study. Significant lipids in serum were subsequently subjected to Lipid Pathway Enrichment Analysis (LIPEA) [71].

For the target screening of BAs, concentrations of the detected BAs were calculated by interpolating the constructed IS-calibrated linear-regression curves of individual BAs, with the peak area ratios measured form injections of the sample solutions. TraceFinder 5.2 General Quan (Thermo) was employed for this analysis. GraphPad Prism (version 10.1.0) was used to perform ANOVA with Tukey's HSD and graphs.

2.4.2. Metagenomic analyses and omics integration

The Integrated Meta-omic Pipeline [72] (IMP; v3.0 commit# 9672c874; available at GitLab [73]) was employed to process paired and reverse reads using the metagenomic workflow with default settings. As part of the workflow, metagenomic reads aligning with the human genome were filtered and removed. Taxonomic profiles were generated using mOTUs (v2.0). Furthermore, reads were assembled into contigs, which were used for gene predictions using Prokka [74], and subsequently annotated using the Kyoto Encyclopedia of Genes and Genomes (KEGG) orthologous categories. The KEGG orthologous (KO) genes were identified, and their coverages based on number of reads mapping to individual KOs were used for subsequently analyses.

The mOTU table was normalized by the total sequence count following which MicrobiomeAnalyst 2.0 [75], [76], marker data profiling option, was employed to filter based on a prevalence threshold of 30% across samples (minimum count requirement of one), and to compute alpha-diversity and core microbiome composition. In addition, the ampvis2 [77] R package was employed for data visualization purposes. As for the metabolomics/exposomics data, ANOVA test was computed in R and a p-value <0.05 was considered statistically significant.

For the KOs, Transcripts Per Kilobase Million (TPM) were calculated in R, accounting for sequencing depth per sample and gene lengths. Pathways from the significant KOs were obtained via the KEGGREST [78] package in R, see the GitLab repository for details [62]. To provide a comprehensive overview, TPM values of KOs sharing the same pathway were summed and ANOVA was performed to identify the statistically significant pathways across groups.

The normalized abundance mOTU table (metagenomics) and normalized peak intensities table (metabolomics/exposomics) were integrated using Data Integration Analysis for Biomarker discovery using latent components (DIABLO) within the mixOmics [79] package in R. Details about this analysis are available in the GitLab repository [62]. Spearman's correlation between the mOTUs and chemicals was computed in R, using the cor.test function of the base R stats package, while the Corrplot package, was used to perform the correlation plots.

The MultiGroupPower function from the MultiPower R package [80], [81] was applied to compute the power calculations integrating the metabolomic/exposomic and metagenomic datasets, derived from the dust analysis.

2.5. Neuronal differentiation and Bisphenol S (BPS) exposure

2.5.1. Generation of midbrain dopaminergic neurons

Induced pluripotent stem cells (iPSCs) were obtained from a PD individual carrying the *LRRK2* G2019S variant. An isogenic control (IC) was engineered from the same line using CRISPR-Cas9 technology [82], [83], [84]. Neuronal cultures enriched in midbrain dopaminergic neurons were generated following the Reinhardt *et al.* protocol [83], [85], details can be found in **S1.4.1** and **Table S9.** At day 29, cells were treated for 24 hours with bisphenol S (BPS) (Sigma, 43034), at two different concentrations (100 μM and 500 μM), using dimethyl sulfoxide (DMSO) (Sigma, D2438) as a vehicle, before staining and imaging. Details about the mitochondrial membrane potential and mitophagy assays can be found in **S1.4.2** and **S1.4.3**, respectively.

2.5.2. Image Analysis

Automated image analysis was performed using Matlab (version 2021a, MathWorks), adapting the method detailed in Baumuratov *et al.* [86]. The analysis was performed on the HPC platform [87] from the University of Luxembourg in collaboration with the LCSB Bioimaging platform. Features such as *mitochondrial mass* (sum of mitochondrial pixels/sum of nuclei pixels), *mitochondrial size* (sum of mitochondrial pixels/mitochondrial counts), *mitochondrial membrane potential* (mean intensity of TMRE inside the mitochondrial mask), and *normalized mitophagy* (sum of pixels positive for Mitotracker Green FM and Lysotracker Deep Red/sum of mitochondrial pixels) were extracted.

Statistical analyses and data visualization were performed in GraphPad Prism (version 10.1.0). Comparative analyses were performed using the Kruskal-Wallis test, followed by multiple comparisons with the uncorrected Dunn's test.

3. Results and discussion

3.1. Dust Metabolome and Exposome

3.1.1 Overview of Chemical Composition

The chemical composition of the dust was analyzed by non-target LC-HRMS, using the different cheminformatic approaches described above, resulting in 1,003 annotated chemicals (Level 1-3), with ninety features being statistically significantly different (ANOVA p-value<0.05). **Table S10** contains detailed information about all annotations, including statistical results and MetOrigin classifications, while **Table S11** contains the statistically significant chemicals only. The potential sources of these compounds according to the NORMAN-SLE [34] and PubChem Compound TOC [29] are shown in **Figure 2**, while the MetOrigin [67] classifications are shown in **Figure S9**.

Hundreds of chemicals (784) in dust were found in different lists from the NORMAN-SLE tree (**Figure 2A**). These NORMAN-SLE lists were selected to provide a comprehensive understanding of the types of chemicals annotated in the household dust samples. Most matches (544, of which 51 were significant) were found in the S32 REACH17 [37], which is a list of chemicals registered under REACH, the European Chemical Legislation that requires registration of chemicals in use above one tonne per annum [88]. Benzocaine, benzyl butyl phthalate, and scopoletin are some examples of REACH chemicals found in household dust samples. Notably, 204 out of the 1,003 chemicals identified in this study were previously noted in the NORMAN collaborative household dust trial [26] (S35 INDOORCT16 list [39]). These included plasticizers such as dibutyl phthalate, pharmaceuticals such as tramadol, benzocaine, ketoprofen, gabapentin and the fungicide carbendazim, one of the most prevalent biocides in Italian household dust samples [89]. Furthermore, 151 chemicals were potential ingredients of cosmetics, mapping to the S13 EUCOSMETICS [36] list, while 52 were present in the

list of chemicals associated with neurotoxicity (S37 LITMINEDNEURO [38]), including 2,4-dinitrophenol and diethyltoluamide (DEET). Additionally, 89 chemicals associated with plastic packaging (via S49 CPPDBLISTB list [90]) were tentatively identified, including dibutyl phthalate, and bisphenol A diglycidyl ether. The overlap of chemicals across all these lists was high (**Figure 2B**), suggesting that most of the annotated compounds have multiple potential origins and/or reasons for interest.

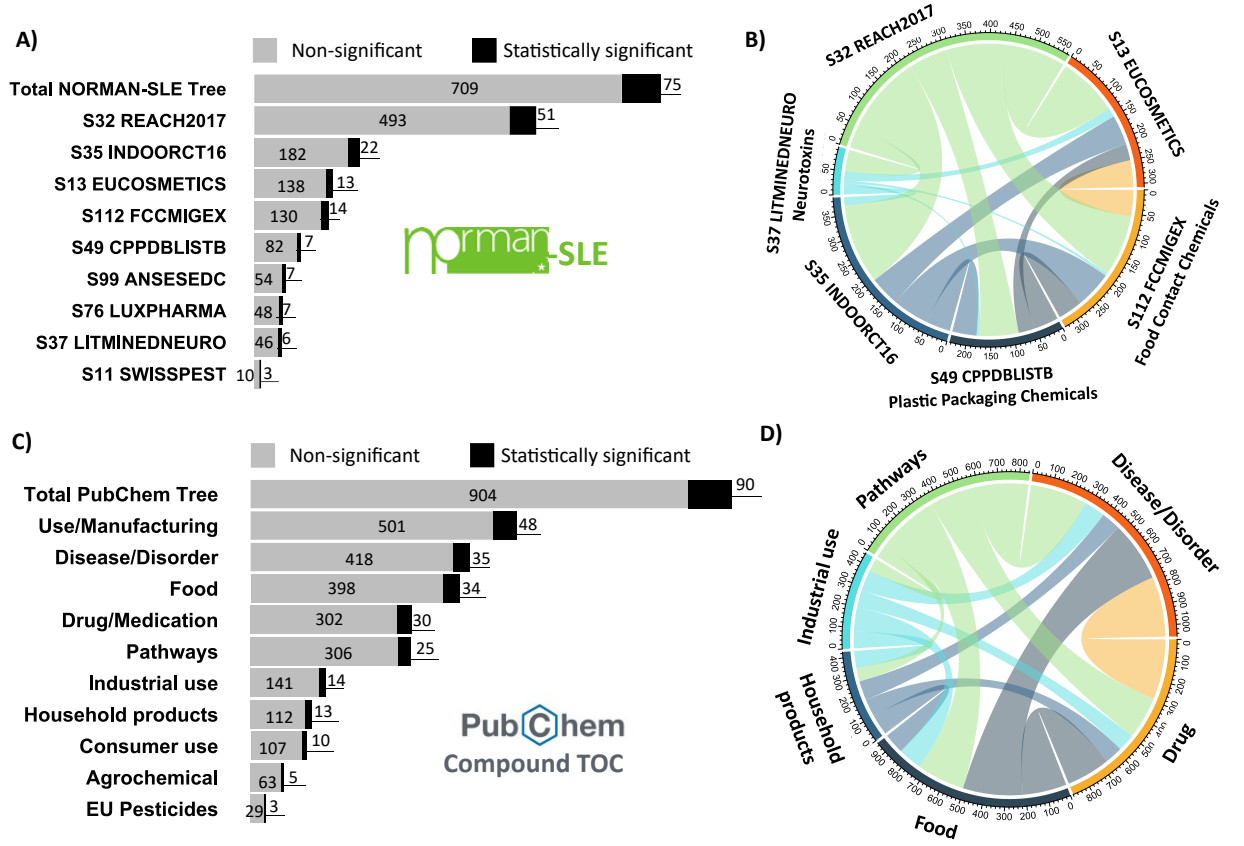

Figure 2. *Potential sources of the identified chemicals in the dust.* ***(A)*** *Selected lists from the NORMAN-SLE tree;* ***(B)*** *Chord diagram displaying the overlap of the different lists;* ***(C)*** *Selected categories from the PubChem TOC;* ***(D)*** *Chord diagram displaying the overlap of different PubChem categories* ***(D).*** *Full results are available in* ***Table S10****. Note that queriers were performed in April 2024.*

Figure 2C shows the potential categories of chemicals based on the PubChem Compound TOC, with overlap in **Figure 2D**. The "Use and manufacturing" category was the most prevalent, with such information available for 549 of the annotated compounds. Disorders and diseases information was associated with 453 compounds, including 4-chloro-3-methylphenol and DEET. Interestingly, 432 chemicals were classified as food by the PubChem Compound TOC (**Figure 2 C**), while 506 chemicals were in this MetOrigin class (**Figure S9A**); 366 of these overlapped. Additionally, 282 chemicals are potentially related to microbiota according to MetOrigin (**Figure S9A**). As for the NORMAN-SLE

categories (**Figure 2B**), the overlap across the different PubChem TOC categories was high (**Figure 2D**).

3.1.2 Relevant Chemicals Potentially Related to Penetrance

Ninety statistically significant chemicals were found across the groups, indicating potential relevance for disease penetrance. **Figure 3** shows the distribution of four of these: bisphenol S (BPS), perfluorobutane sulfonic acid (PFBuS), 2-benzothiazolesulfonic acid ($BThSO_3$) and 2-phenylphenol (2PP). Interestingly, the first two are replacements of hazardous chemicals; BPS (**Figure 3A**) emerged as a "safer" alternative to bisphenol A (BPA) [91], while PFBuS (**Figure 3B**) is a substitute for perfluorooctane sulfonate (PFOS) [92]. All compounds illustrated in **Figure 3** had elevated levels in PD+/LRRK2+ compared to the PD-/LRRK2+ group. Thus, these compounds could be potential targets for further investigations into environmental influences on *LRRK2* penetrance in PD.

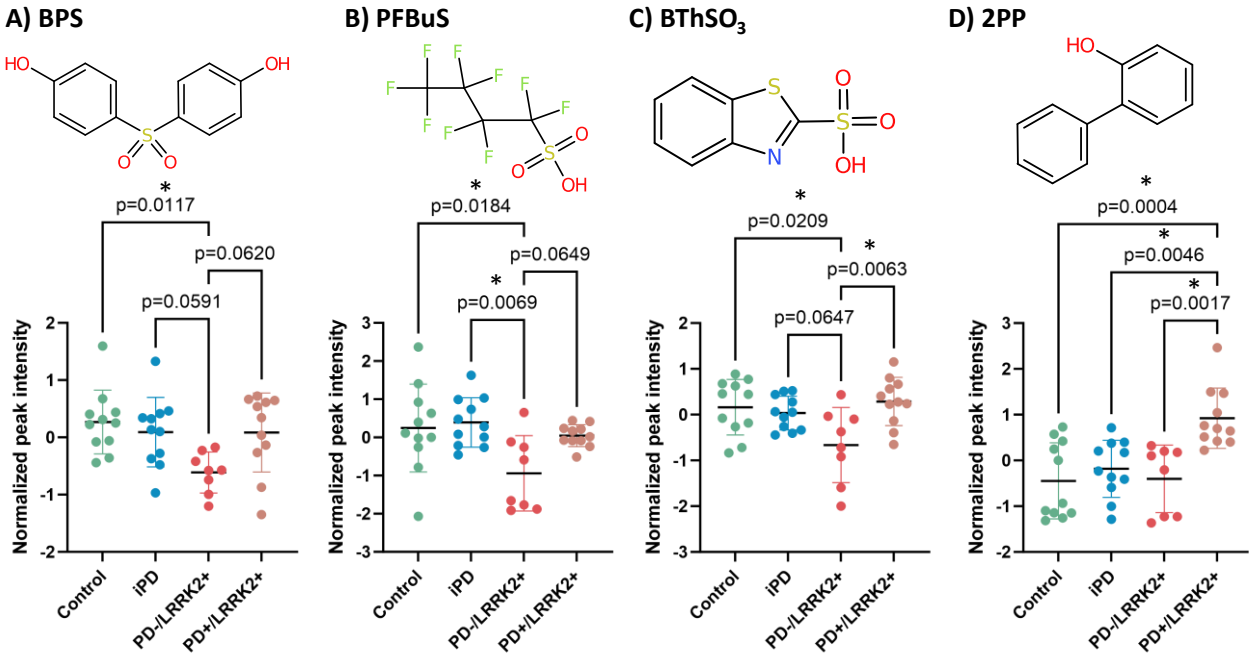

Figure 3. *Normalized peak intensities across groups of* ***(A)*** *BPS; bisphenol S,* ***(B)*** *PFBuS; perfluorobutane sulfonic acid,* ***(C)*** *$BThSO_3$; 2-Benzothiazolesulfonic acid, and* ***(D)*** *2PP; 2-phenylphenol in dust. p= Tukey's HSD post-hoc p-value. Note that p< 0.1 is displayed although only p<0.05 is considered statistically significant here (marked with an "*").*

Significantly higher levels of BPS were found in the control group compared to the PD-/LRRK2+. Higher levels of BPS were also observed in the PD+/LRRK2+ group compared to the PD-/LRRK2+ group (**Figure 3A**). Two other bisphenol species, bisphenol P and bisphenol A diglycidyl ether (**Figure S10**), were also annotated in the dust samples, albeit not found to be statistically significantly different. BPS has been employed extensively in industry to produce BPA-free products. However, BPS can have

similar or even greater toxicity than BPA [93], exhibiting stronger reproductive effects, DNA damage, longer bioavailability, and better dermal penetration compared with BPA [94]. Additionally, BPS exhibits higher resistance to biodegradation, rendering it more prone to accumulate and persist in the environment [91]. It can disrupt lipid metabolism, glucose metabolism, nucleotide metabolism, vitamin metabolism, and induce oxidative stress [94]. BPS can cross the blood brain barrier (BBB) [95] and may trigger neurotoxicity through different pathways, potentially posing a risk factor for the development of neurodegenerative diseases including PD [91], [94]. Therefore, this compound was tested in cell-based models (neurons), to investigate its potential neurotoxic effects, as discussed in **Section 3.5.**

The dust analysis revealed significantly lower levels of PFBuS (**Figure 3B**) in the PD-/LRRK2+ participants compared to the iPD and control groups, while a similar lower trend was found in PD-/LRRK2+ group compared with PD+/LRRK2+. PFBuS is a per-/polyfluoroalkyl substance (PFAS), which is a group of substances of high environmental and toxicological concern due to their long-term environmental persistence and toxicity to organisms, including humans [96]. PFBuS, a relatively short-chain PFAS, is currently used as substitute for PFOS due to lower toxicity and bioaccumulation [92], [97]. However, adverse effects including cytotoxicity, endocrine disruption, immunotoxicity, reproductive toxicity, hepatotoxicity and neurotoxicity have been associated with PFBuS [92], [97]. PFBuS can cross the BBB, affecting the Central Nervous System (CNS). While PFBuS is considered less toxic than PFOS, both compounds exhibited similar mechanisms of toxicity in zebrafish models [97].

Ten additional PFAS were annotated in dust, including the pesticide fipronil and its transformation products fipronil desulfinyl and flipronil sulfone, which were mainly found in one patient from the iPD group (**Figure S11A-C**). Fipronil, a PFAS-containing pesticide subject to stringent regulations in Europe due to its potential environmental and health-related risks, was (unexpectedly) identified in the dust samples. Although the use of fipronil in food production for human consumption was banned in Europe in 2013, eggs contaminated with fipronil were found in the Netherlands and neighboring countries in 2017 [98], [99]. The veterinary application of fipronil emerged as a significant potential source of this compound in household dust across Europe. Nonetheless, a prior study conducted in Italy in 2016 noted that the highest levels of fipronil were observed in a household dust without pets [100]. These findings, coupled with our observation of fipronil in German household dust, underscore the necessity for continued regulatory interventions in Europe. Fluorometuron (**Figure S11D**), another PFAS-containing pesticide, was also tentatively identified with overall higher peak intensities in the PD-/LRRK2+ dust samples. Additionally, PFAS-containing pharmaceuticals were annotated, including fluoxetine, flutamide, and etofenamate, without significant differences across groups (**Figure S12**). A PFAS with multiple industrial uses, 6:2 fluorotelomer sulfonic acid (6:2 FTSA), had a non-significant lower trend in the PD-/LRRK2+ group compared to the control (**Figure S13A**).

Trifluoromethanesulfonic acid (TFMS), an ultra-short chain PFAS, showed statistically higher levels in the dust from the PD+/LRRK2+ group compared to the PD-/LRRK2+ (**Figure S13B**).

2-Benzothiazolesulfonic acid ($BThSO_3$) was found at statistically significantly lower levels in the PD-/LRRK2+ group compared to the PD+/LRRK2+ (**Figure 3C**). This trend was also consistent with its transformation product, 2-hydroxybenzothiazole (OBTh), as shown in **Figure S14A**. Benzothiazole (BTh), a parent compound of OBTh, 2-(4-morpholinyl)benzothiazole (24MoBTh), and 2-aminobenzothiazole (ABhT) were also detected in the dust samples, without being statistically significantly different (**Figure S14B-D**). Benzothiazoles (BThs) have multiple applications, including as vulcanization accelerators in rubber manufacture, fungicides, antialgal agents, slimicides, chemotherapeutics and corrosion inhibitors [101]. BThs undergo chemical, biological and photodegradation in the environment, leading to the formation of several transformation products [102], as shown in **Figure S15** and discussed later (**Section 3.3**). Previous studies have associated BThs with different toxic effects, including carcinogenicity [102], [103], [104] and impaired child neurodevelopment due to prenatal exposure [105]. However, the environmental exposure to these compounds and the long-term consequences are presently unresolved.

2-Phenylphenol (2PP), an antimicrobial agent used in household products and included in the European Union pesticides database, was found with statistically significantly higher levels in the PD+/LRRK2+ group compared with the three others (**Figure 3D**). 2PP was previously found in household waste [106], food and dairy products [107] and cosmetics (S13 EUCOSMETICS list [36], as illustrated in **Figure 2A**). It is also listed as a potential endocrine disruptor in the S109 PARCEDC list of potential endocrine disrupting compounds [108]. Moreover, a recent rat-based study showed that the exposure to this compound altered phospholipid, fatty acids, sterol lipid, and amino acid levels [109].

While four chemicals have been discussed in more detail here due to their relevance as potential neurotoxic compounds in the environment and for space reasons, another 86 compounds were found to be statistically significant across groups, as detailed in **Table S11**.

3.2. Differentially Abundant Taxa and Microbial Gene Signatures

To complement the dust-derived metabolomics/exposomics, the microbial communities of the dust samples were analyzed at different taxonomic ranks (from kingdom to species). A total of 1,782 metagenomic operational taxonomic units (mOTUs) were initially characterized (**Table S12**). This initial list was reduced to 163 mOTUs for subsequent analysis (**Table S13**), after filtering to remove low quality or uninformative features, as indicated in the Material and Methods section. Notably, *Actinobacteria*, *Proteobacteria,* and *Firmicutes* emerged as the three most abundant phyla (**Figure 4A**).

The dominance of these phyla in household dust aligns with multiple previous studies [28], [110], [111]. *Actinobacteria* spp. were found with the highest abundance in the iPD dust samples, matching observations in previous studies showing this genus to be enriched in feces from PD patients [3], [112].

The core microbiome at the species level was investigated (**Figure 4B**), with *Cutibacterium acnes* the most prevalent species. This shows the significant biological components of the dust, including skin cells. Interestingly, lower alpha-diversity was noted in the iPD group (phylum level) compared to the control group (**Figure 4C-D**). However, no statistically significant differences were observed in the alpha-diversity at species level (**Figure S16**), aligning with previous studies which reported no significant differences in the alpha-diversity in the feces of PD patients compared to the control participants [3], [112].

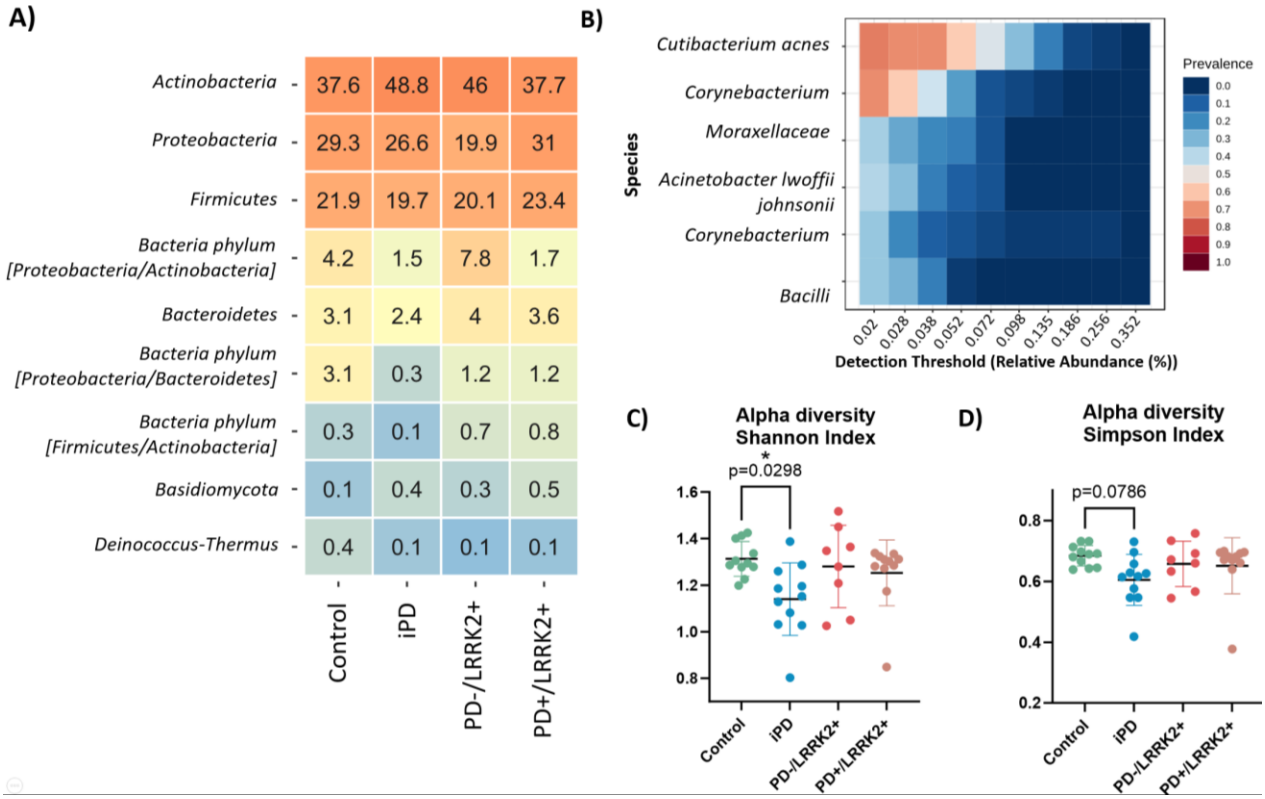

Figure 4. *(A) Heatmap showing the most abundant phyla entries from the "Phylum" column of the filtered mOTUS (**Table S13**). (B) Core microbiome showing the most abundant species entries from the "Species" column (**Table S13**). (C) Box plot showing the alpha-diversity across groups with Shannon Index and (D) Simpson Index at phylum level. p= Tukey's HSD post-hoc p-value. Note that p< 0.1 is displayed although only p<0.05 is considered statistically significant here (marked with an "*").*

Ten mOTUs were differentially abundant across groups (p< 0.05, ANOVA; **Table S13** and **Figure S17**), including *Clavibacter michiganensis, Marmoricola sp. Leaf446*, three different species of

Nocardioides and *Sphingomonas, Candidatus Rickettsiella isopodorum,* and *Acinetobacter parvus*. Intriguingly, for all these mOTUS, the PD-/LRRK2+ group showed the lowest abundances. *Clavibacter michiganensis* (**Figure S17A**), recognized as a plant pathogen [113], demonstrated a significant increase in the iPD group compared to the control and PD-/LRRK2+ groups. The same trend was observed for *Marmoricola sp Leaf446.* (**Figure S17B).** This species has been mainly isolated from environmental sources, however a previous study found the *Marmoricola* genus to be highly abundant in the nasal microbiota of PD patients compared to control individuals [114]. *Nocardioides* (**Figure S17C-E**), was found elevated in the iPD group compared to the PD-/LRRK2+. Of note, *Nocardioides* spp. can degrade a wide range of organic pollutants such as nitrophenol, ibuprofen, cotinine, melamine, or atrazine. Furthermore, *Nocardioides* can carry out steroid biodegradation and biotransformation [115]. *Sphingomonas* spp. (**Figure S17F-H**), was found significantly higher in the dust samples from the iPD compared to the PD-/LRRK2+ group. Interestingly, a previous study reported higher abundances of *Sphingomonas* genera in feces samples from PD patients, compared to a healthy control group, associated this with motor complications [116]. *Candidatus Rickettsiella isopodorum* (**Figure S17I**), an intracellular bacterium infecting terrestrial isopods [117], was significantly higher in the control group. Lastly, statistically significantly elevated abundances of *Acinetobacter parvus* (**Figure S17J**) were observed in the PD+/LRRK2+ group compared to the others. This is an opportunistic pathogen associated with nosocomial infections.

In addition to the differentially abundant taxa, a total of 14,444 different KOs were characterized, of which 624 were statistically significant across groups. Pathways from the significant KOs were obtained, resulting in 269 KEGG pathways (**Table S14**) of which 207 were statistically significant. **Figure 5** illustrates the distribution of some of those pathways across groups, whereby the top thirty statistically significant pathways are represented in **Figure S18**. Notably, "microbial metabolism in diverse environment", "carbon metabolism" and "glyoxylate and dicarboxylate metabolism" pathways were increased compared to the control and iPD groups, compared to the PD-/LRRK2+ and PD+/LRRK2+ groups (**Figure 5A-C**). Furthermore, arginine, proline, phenylalanine, and butanoate metabolism exhibited the same trend, *i.e.*, significatively decreased in PD-/LRRK2+ compared to the control and iPD groups (**Figure S19**). In contrast, an increase in ribosomal genes was observed in PD-/LRRK2+ and PD+/LRRK2+ groups, suggesting that dust-borne bacteria might be compensating the lower metabolism (**Figure 5D**). Finally, both beta-lactam and vancomycin resistance appear to be elevated in PD-/LRRK2+ and PD+/LRRK2+ (**Figure 5E-F**). Overall, the pathways results (**Figure 5**) show similar trends between control and iPD groups, and between PD-/LRRK2+ and PD+/LRRK2+. This suggest that the indoor microbial environment was similar in the participants carrying pathological variants of *LRRK2*.

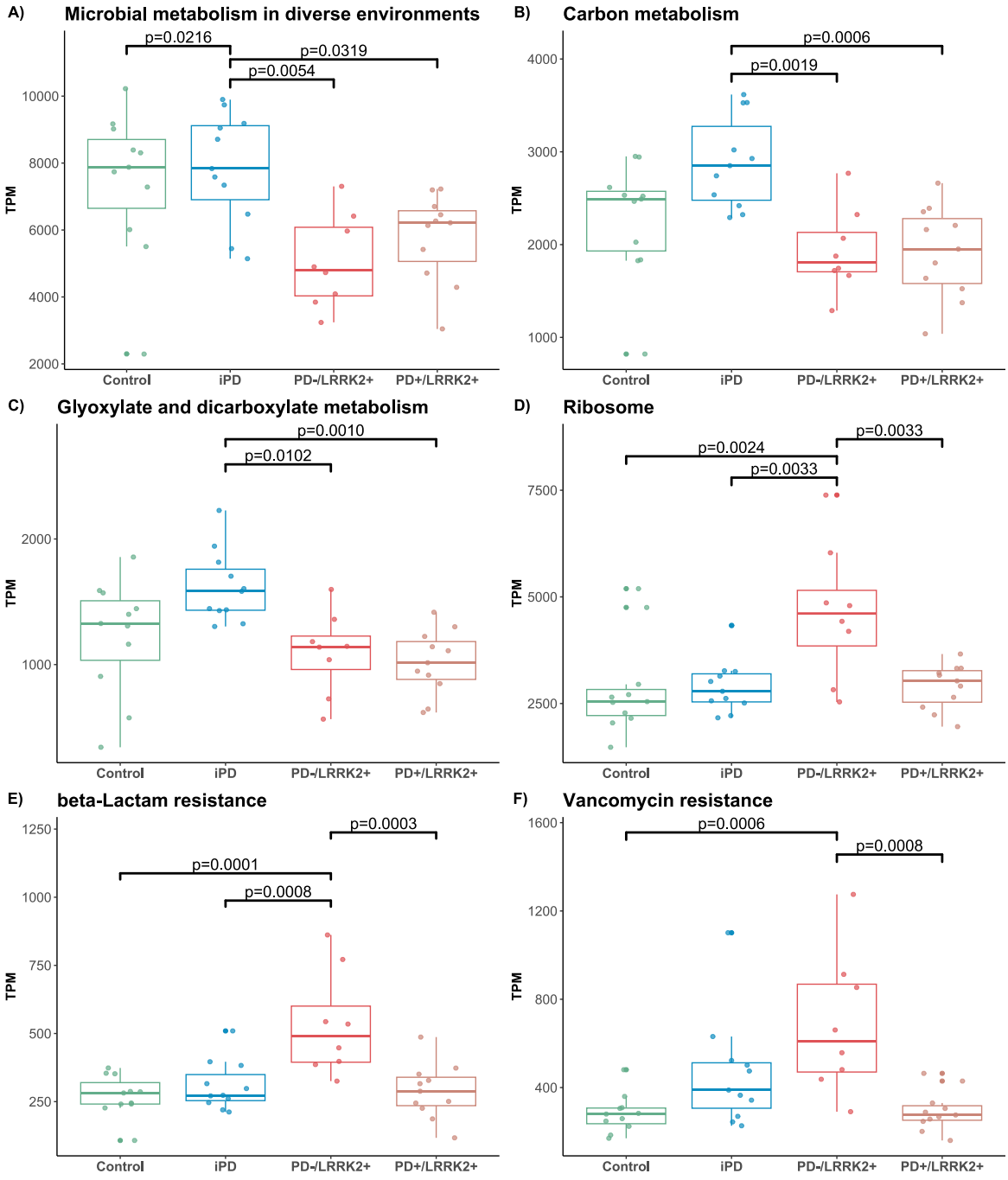

Figure 5. *Bar plots of some of the significant KEGG pathways found in the dust samples. Note that TPM values of the KOs sharing the same pathway were summed. p= Tukey's HSD post-hoc p-value. Abbreviations: TPM; Transcripts Per Kilobase Million, KOs; KEGG orthologous genes.*

3.3. Dust Omics Integration

Two different approaches were employed to investigate the potential relationships between the chemicals and the microbiome constituents found in the household dust: (1) DIABLO, a framework

used to integrate the datasets of chemicals (**Table S10**), and mOTUs (**Table S13**) (**Figure 6A-B**); and (2) Spearman correlation analysis, employed to explore in detail the potential correlation between some genera (*Rhodococcus* spp., *Pseudomonas* spp., and *Arthrobacter* spp.) and benzothiazoles (**Figure 6C**). The DIABLO analysis (**Figure 6A**) indicated that PD-/LRRK2+ clustered separately from the rest of the groups (left), while some iPD and control samples cluster together (right). This classification is mainly driven by the metabolomics/exposomics data, as most of the selected features are chemicals. Interestingly, two of the selected features are PFAS, PFBuS and 6:2 FTSA, which have lower levels in the PD-/LRRK2+ group compared to the controls, as previously indicated (**Figure 3B** and **Figure S13A**). Sample plots from the final DIABLO model in **Figure 6B** display the degree of agreement between the two datasets. Importantly, the PD-/LRRK2+ samples clustered together in both metabolomics and metagenomics datasets.

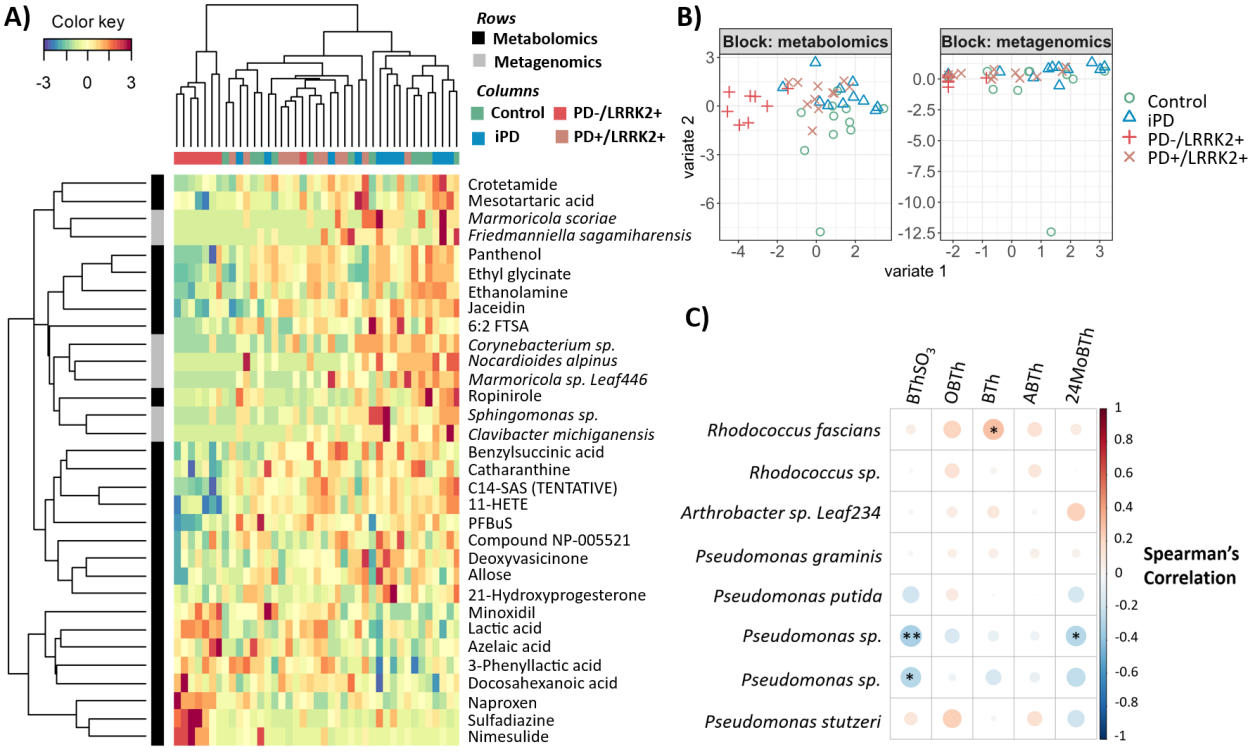

Figure 6. *(A) DIABLO Clustered heatmap showing the variables selected by multiblock sPLS-DA performed on the metagenomics (mOTUs table) and metabolomics/exposomics (peak intensities table) dust datasets on component 1. Samples represented in columns and features in rows.* ***(B)*** *DIABLO sample plot showing the discrimination across groups based on metabolomics (left panel) and metagenomics data (right panel).* ***(C)*** *Spearman's correlation analysis between Rhodococcus* spp. *and benzothiazoles. Red color indicates positive correlation while blue color indicates negative correlation. The size of the dots is proportional to the absolute value of the correlation coefficient. ** p-value<0.05 *p-value<0.1. Abbreviations: 6:2 FTSA; 6:2 fluorotelomer sulfonic acid, PFBuS; perfluorobutane sulfonic acid, BThSO$_3$; 2-Benzothiazolesulfonic acid, OBTh; 2-hydroxybenzothiazole, BTh; benzothiazole, ABTh; 2-Aminobenzothiazole, and 24MoBTh; 2-(4-Morpholinyl)benzothiazole.*

Certain species within the genus *Rhodococcus* have been reported to degrade $BThSO_3$ (**Figure 3C**) to OBhT (**Figure S15**) [101], [102]. Furthermore, BTh can be degraded by several bacterial species including *Rhodococcus* sp., *Pseudomonas* sp., *Arthrobacter* sp. and *Enterobacter* sp. [102]. Interestingly, all of these were identified in the dust samples, although only the first three species were included in the filtered dataset (**Table S13**).

Spearman's correlation analysis was subsequently performed between all the BThs identified in the dust samples (**Figure 3C** and **Figure S14**), and *Rhodococcus, Pseudomonas,* and *Arthrobacter* species, known for their capacity to degrade specific BThs [101], [102]. A negative and statistically significant association was observed between *Pseudomonas* sp. and $BThSO_3$ (**Figure 6C**). The same negative association was found between *Pseudomonas* sp. and 24MoBTh, suggesting that this species may degrade both $BThSO_3$ and 24MoBTh. Intriguingly, our analysis unveiled a positive (p-value<0.1) association between BTh and *Rhodococcus fascians*. This association may be explained by several factors, including photodegradation or microbial degradation (e.g., by *Pseudomonas*) of other compounds such as 24MoBTh leading to the formation of BTh. Additionally, the presence of multiple microorganisms and chemicals in the household dust samples may influence the growth of *Rhodococcus fascians* and/or BTh metabolism. Therefore, further studies in controlled environments are necessary to provide more insights into the relationship between *Rhodococcus fascians* and BTh in household dust samples.

Overall, these results demonstrate agreement between both omics approaches as they effectively discriminated the same group (PD-/LRRK2+). Furthermore, the findings suggest a potential relationship between chemicals and microbes, indicating that some of the chemicals found in dust may be metabolized by microbes.

3.4. Serum Metabolome, Exposome, and Lipidome

The analysis of dust samples was complemented by exploring the serum of some participants where matched samples were available. This included a non-target screening of polar chemicals (**Table S15**) and lipids (**Table S16-17**), as well as the quantitative target screening of BAs (**Table S18**).

3.4.1 Polar Chemicals in Serum

Forty-nine chemicals were annotated (Level 1-3) in the polar fraction of the serum samples, with three statistically significant results (1,7-dimethyluric acid, pipecolic acid, and amantadine). After data normalization, the PCA plot (**Figure S20**) displayed all the QC samples with a tight clustering. This

indicates that the instrument variation was effectively corrected, affirming a good system stability and reliability of the results.

1,7-Dimethyluric acid, a metabolite of caffeine, was elevated in the control and PD-/LRRK2+ groups compared with the PD+/LRRK2+ group. Although this metabolite was not found in the dust, the parent compound (caffeine) was identified, without significant differences but with an average higher normalized peak intensity in the control group (**Figure S21**). These results agree with previous studies [118], [119], which proposed lower levels of caffeine and caffeine metabolites as potential diagnostic biomarkers for early PD. Caffeine, a common psychostimulant, has shown neuroprotective effects (via reduction of Reactive Oxygen Species (ROS)) and appears to improve motor symptoms in PD [118], [119]. Lower levels of caffeine and its metabolites in PD patients might be explained by a malabsoption in the small intestine. Although microbiome dysbiosis is a common feature in PD, to date it remains unclear whether caffeine malabsorption in PD is influenced by this [119].

Pipecolic acid was found significantly lower in the PD+/LRRK2+ group compared to the iPD group. This compound was also identified in the dust samples, without being statistically significantly different (**Figure S22**). Interestingly, opposite trends were observed, which suggests that biological samples do not always reflect environmental exposures. A previous study reported decreased levels of pipecolic acid in plasma samples from pre-PD individuals, suggesting that this may be indicative of microbiota-gut-brain axis (MGBA) dysregulation [120]. Pipecolic acid can be produced by intestinal bacteria and cross the BBB [121], where it can act as a neurotransmitter, modulating the uptake of γ-aminobutyric acid (GABA) by brain neurons [120], [122]. Moreover, pipecolic acid may originate from the breakdown of lysine in human mitochondria and peroxisomes, which are organelles involved in many roles including β-oxidation metabolism, and ROS homeostasis [120], [122]. Dysfunction of these organelles contributes to the aging process and neurodegenerative diseases, including PD [123].

Amantadine is an antiviral and antiparkinson drug, which was exclusively found in the two PD groups (iPD and PD+/LRRK2+), as expected. This trend was consistent for both dust and serum samples (**Figure S23**). Furthermore, levodopa, the most commonly prescribed medication for first-line therapy in PD, was found solely in the household dust of PD participants (iPD and PD+/LRRK2+, **Table S10** for details) [6]. Importantly, the intake of amantadine, levodopa, and other dopaminergic drugs

(exclusively in the PD groups) may influence the metabolism, and consequently the observed results in the serum samples.

3.4.2 Serum Lipidome

A total of 313 unique lipids were annotated (Level 2-3) in the serum samples by non-target LC-HRMS analysis (**Table S16**), with 252 in ESI (+) and 61 in ESI (-), see **S2.3** and **Figure S24-25** for details about the filtering and quality control approaches. The most abundant lipid categories in serum included glycerophospholipids, glycerolipids and sphingolipids. Forty-three lipids were statistically significantly different, primarily glycerophospholipids (34 of 43; **Figure S24**). Lipid pathway enrichment analysis, computed with the significant lipids, revealed glycerophospholipid metabolism and sphingolipid metabolism as the most altered pathways (**Table S17**), which is consistent with a previous study performed in serum samples from PD and *LRRK2* carriers [124].

Among the glycerophospholipids, phospathidylcholines (PCs) were significantly decreased in the PD+/LRRK2+ or PD-/LRRK2+ compared to the other groups under study (**Figure S26** and **Table S16**). A significant decrease of PC 14:0_18:2 was observed in the PD+/LRRK2+ compared with the PD-/LRRK2+ and iPD groups. PCs are the most abundant glycerophospholipids in membranes and are involved in the control of inflammation, neuronal differentiation and cholesterol homeostasis [125], [126]. Thus, a decrease in PCs may contribute to the neuroinflammation and disease progression, as previously suggested [125]. In contrast, some lysophosphatidylcholines (LPCs), breakdown products of PCs, were significantly elevated in the PD+/LRRK2+ group, including LPC 18:1 and LPC 16:0 (**Figure 7A-B**). This is in line with a previous study [125], suggesting that alterations in LPCs serve as markers of mitochondrial dysfunction, neuroinflammation and oxidative stress processes. Additionally, lysophosphatidylethanolamines (LPEs), LPE 18:0 and LPE O-18:1 (**Figure 7C-D**), were significantly elevated in the PD+/LRRK2+ group compared with the control group. This in contrast with previous studies performed in plasma [127] and serum [125] of iPD participants, which found decreased levels of LPE with the advance of the disease. Thus, it would be interesting to check further whether this alteration is specific to patients carrying *LRRK2* pathogenic variants. Previous studies have shown that the BPS exposure in adipocytes [128] and macrophages [129] induce lipidome changes including increased levels of PCs, LPCs, and LPEs.

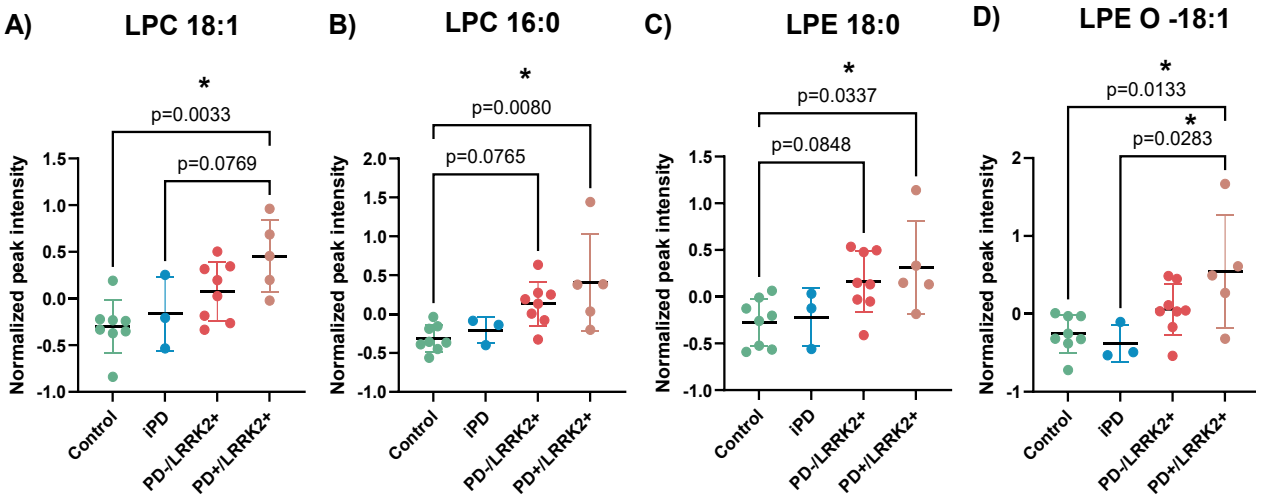

Figure 7. *Bar plots showing the normalized peak intensities across groups of LPC 18:1* ***(A),*** *LPC 16:0* ***(B),*** *LPE 18:0* ***(C),*** *and LPE 0-18:1* ***(D).*** *p= Tukey's HSD post-hoc p-value. Note that p< 0.1 is displayed although only p<0.05 is considered statistically significant here (marked with an "*").*

The quantitative analysis of BAs in serum did not reveal any statistically significant differences (**Table S18**), which is in contrast with recent work on Alzheimer's disease progression in cerebrospinal fluid (CSF) samples [130]. However, non-significant higher trends of the neuroprotective BAs chenodeoxycholic acid (CDCA), and ursodeoxycholic acid (UDCA) were observed in PD-/LRRK2+ in comparison to the PD groups (**Figure S27A-B**). Higher but non-significant trends of the cytotoxic BA deoxycholic acid (DCA) were also observed in the PD-/LRRK2+ group (**Figure S27C**). Previous research has reported elevated levels of secondary cytotoxic BAs in PD, including DCA and lithocholic acid, correlated with an increase in BA-metabolizing bacteria [2], [49]. Thus, the non-significant higher trends of BAs found in the PD-/LRRK2+ and iPD groups may be explained by gut microbiome dysbiosis, as the gut microbiota metabolize the primary BAs to produce secondary BAs such as DCA [49]. However, this was not investigated further here due to the lack of significance. Since BAs are crucial signaling molecules and key modulators of metabolism and immune homeostasis [131], investigating BAs in future studies with larger sample sizes could provide additional insights.

3.5. Effects of BPS on Neurons

While the vast majority of studies on BPS so far have focused on its endocrine disrupting effects [91], recent findings have linked this chemical to an elevated risk of neurodegenerative diseases [132]. The potential neurotoxic effect of BPS found in the dust samples here (**Figure 3A**), in the context of LRRK2-based PD, was explored in cultures enriched with dopaminergic neurons generated from a PD individual carrying the *LRRK2* G2019S variant and its isogenic control (IC), as shown in **Figure 8A**.

Exposure to BPS elicited distinct responses in the IC and PD+/LRRK2+ neurons, particularly at the level of mitochondrial homeostasis. Functional evaluation of mitochondria upon BPS exposure showed that the IC neurons respond by elevating the mitochondrial potential, a response not seen in the PD+ cells (**Figure 8B**). This may be interpreted as a compensatory response of IC neurons to increase ATP production, or conversely, as a result of mild ATP-synthase inhibition, which leads to hyperpolarization of mitochondrial membrane potential due to lower consumption of the mitochondrial proton gradient. Disparate effects of BPS treatment were also observed in the averaged mitochondrial mass, i.e., the volume of mitochondria per cell. Contrarily to the IC, the PD+/LRRK2+ neurons significantly increased their mitochondrial mass (**Figure 8C**), suggesting that the PD cells accumulate mitochondria due to an impaired mitochondrial clearance mechanism, as previously reported for PD+/LRRK2+ murine models [133]. Alternatively, the cells may intensify mitochondrial biogenesis to compensate for the BPS-induced insult. Furthermore, BPS negatively impacted (reduced) the organellar size in the PD+/LRRK2+ neurons (**Figure 8D**), a response commonly seen upon mitochondrial stress, and which is necessary for efficient clearance via mitophagy to occur. Interestingly, BPS had the opposite effect in the IC line at 100 μM, with an increased mitochondrial size detected. Finally, the proposed alterations in mitophagy were supported by the assessment of the normalized colocalization of mitochondria and lysosomes, which suggests that IC neurons more efficiently initiate this clearance process (**Figure 8E**), and are therefore able to maintain higher mitochondrial fitness. Further experiments, beyond the scope of this current effort, are ongoing to better understand the impact of BPS exposure on neurons.

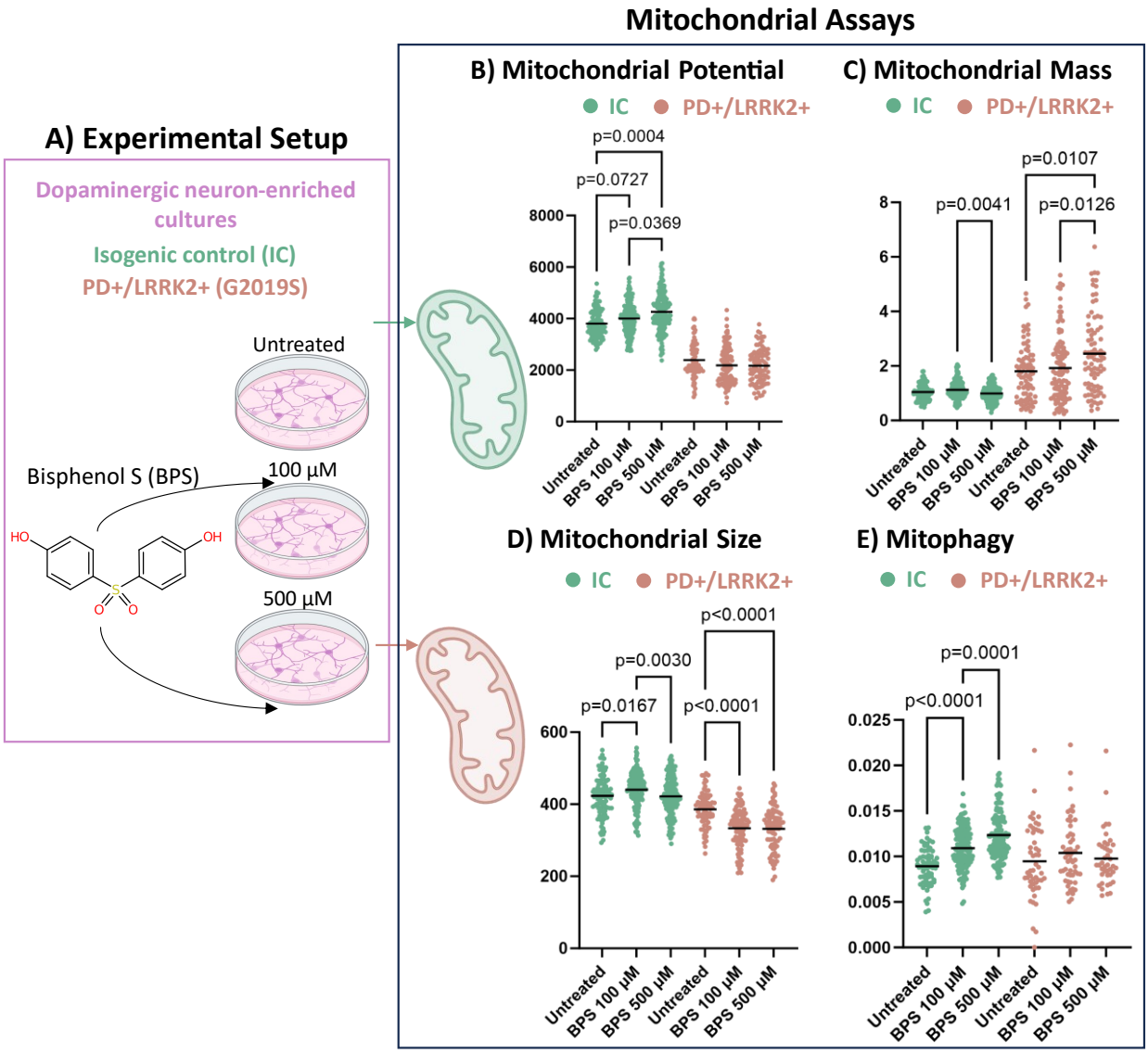

Figure 8. *(**A**) Experimental setup showing the three different conditions for the two groups (PD+/LRRK2+ and isogenic cell lines); untreated, treated with 100 µM of Bisphenol S (BPS) and treated with 500 µM of BPS. (**B**) mitochondrial potential, (**C**) mitochondrial mass, (**D**) mitochondrial size, and E) normalized mitophagy. Kruskal-Wallis test followed by post-hoc Dunn's test (uncorrected) was performed. Dunn's test p-values are displayed in the scatter plots.*

4. Conclusions and future perspectives

Pilot studies, such as this one, play an important role in health research to develop, assess, and adapt the methods employed, generate hypotheses and provide information for a sample size calculation for a larger trial [134], [135]. Using the results generated in this study, a power analysis was undertaken using the MultiPower method in R [80], [81] to calculate the optimal sample size for each group comparison integrating both metabolomics/exposomics (1,003 chemicals, **Table S10**), and metagenomics (163 mOTUs, **Table S13**) datasets to help scope future studies. For an average statistical power of 0.8, the estimated minimum sample size for each group in metabolomics/exposomics ranges between 40 and 89, while for metagenomics it is 36-79. The overall optimal sample size would thus be 273 (**Table S19** for details), and the minimum sample size required per group comparison and omic dataset (metabolomics and metagenomics) is shown in **Figure S28**, which is a challenge for specialized cohorts such as this one.

In this pilot study several significant differences were found in the indoor dust chemical and microbial composition across study groups. Although previous studies have indicated that household dust acts a reservoir of several chemicals and microbial taxa that may pose a risk to human health [24], [26], [136], to our knowledge, the present study represents one of the early substantial efforts to investigate the dust metabolome/exposome and microbiome in the context of PD, and more specifically in PD associated with the penetrance of *LRRK2* pathogenic variants. BPS, PFAS, and BThs showed significantly higher levels in the PD+/LRRK2+ group compared with the PD-/LRRK2+ and should be investigated further (with a larger sample size) to determine whether they could be potential modifiers of *LRRK2* penetrance associated with PD. Moreover, several taxa and KOs were significantly different between groups, with various species (e.g., *Clavibacter michiganensis* and *Marmoricola sp. Leaf446*) displaying significantly lower abundances in the PD-/LRRK2+ group compared to the iPD group (**Figure S17**). In line with previous reports based on the nasal microbiota from PD patients [114], it is worth investigating whether the household environment could be responsible for some of the observations in the host microbiome in future studies. Since oral ingestion of dust is a potential source of exposure to environmental contaminants, especially concerning for infants/toddlers, the connection between dust and the oral-gut axis [137] could be of interest for future investigations.

Differences in the serum lipidome and metabolome were observed, partially matching previously published works. However, most of the chemicals found in dust, which may be potential risks for human health, were not found in the serum samples. This may be because exogenous chemicals are present at trace levels in biological samples compared with endogenous chemicals [138]. Importantly, some of the differences observed in both dust and serum may be due to confounding factors. For instance, the use of medication in the PD groups may influence the metabolism (although no clear relationship was found here), while discrepancies in sample size and age between certain groups, may

influence the results. The average age of the PD-/LRRK2+ group is ten years younger than PD+/LRRK2+, which means that some patients may still develop PD at a later stage. However, it was not possible to get a better match of ages with the samples available in the cohort at this stage.

This study has provided valuable insights for both collecting additional patient information as well as designing future sample collection procedures that will enable better consideration of relevant lifestyle factors in the next investigations. While improving dust sample collection is a subject under discussion, it is logistically much easier for cohorts to obtain samples from household vacuum cleaners (with all the additional variability that this collection method brings due to different brands and bags) rather than deploy more advanced collection systems, which require training of both nursing staff and participants, and make consistent application more challenging. Alternative collection procedures are currently being tested with this cohort in other studies. While this current effort involved samples primarily from Germany, it also included a limited number of samples from Turkey to ensure sufficient sample numbers. As the cohort develops and more samples become available, it will be easier to form more geographically consistent sample sets (in addition to better age matching between groups), which will also ease the data interpretation. Nevertheless, this work has provided a vital basis upon which to design future experiments. Additional insights are being gained through the participation in relevant collaborative trials run by the NORMAN Network, including a second dust trial, which is in the concluding phases, as well as the recently initiated NORMAN indoor air trial.

Finally, this study demonstrated that BPS, a compound found in the household dust samples with statistically significant differences between groups, negatively affected mitochondrial function in PD+/LRRK2+ neurons, providing avenues for further investigation. This underscores the importance of exposome studies in prioritizing chemicals for further exploration with in vitro models.

Supplementary Material

PDF File (Supporting_information.pdf): Contains supplementary material and methods (Section S1, Figure S1-S8) and results (Section S2, Figure S9-28).

Excel file (Supporting_information.xlsx) includes Table S1-S19.

- Table S1-S9: Supplementary material and methods.
- Table S10-S19: Supporting results tables.

Data Availability

The code functions and files associated with this manuscript are provided in the ECI GitLab repository:

https://gitlab.com/uniluxembourg/lcsb/eci/pd-lrrk2

Declaration of competing interest

The authors declare that they have no known competing financial interests or personal relationships that could have appeared to influence the work reported in this paper.

Ethics declarations

The studies involving human participants were reviewed and approved by the Ethics Board of the University of Lübeck (Germany) "ProtectMove (FOR 2488)" and the Luxembourg Comité National d'Ethique de Recherche of Luxembourg.

CReDiT authorship contribution statement

BTA: Writing - Original Draft (lead), Writing – Review & Editing (lead), conceptualization, methodology (lead), formal analysis, investigation, data curation, visualization. SLP: Writing - Review & Editing, formal analysis, investigation, data curation, supervision. SBB: Writing – Review & Editing, formal analysis, investigation, data curation, supervision. TU: Writing - Review & Editing, investigation, resources. MB: Writing - Review & Editing, resources. SE: Writing - Review & Editing, investigation, resources, supervision. PB: Writing - Review & Editing, resources. AR: Writing - Review & Editing, resources. SH: Methodology, investigation. JG: Methodology, investigation. NB: Writing - Review & Editing, resources. PA: Data curation, software. PW: Writing – Review & Editing, conceptualization, methodology, investigation, resources, funding acquisition, supervision. CK: Writing – Review & Editing, conceptualization, resources, funding acquisition, supervision. AG: Writing – Review & Editing, conceptualization, resources, funding acquisition, supervision. ELS: Writing - Original Draft, Writing – Review & Editing, conceptualization, methodology, investigation, resources, funding acquisition, supervision.

Acknowledgements

We thank the Metabolomics Platform of the LCSB for their support with the LC-HRMS analysis. Floriane Gavotto is acknowledged for performing the target LC-MS analysis of the bile acids and the help during data processing with TraceFinder. Rashi Halder and all the sequencing platform of the LCSB is acknowledged for performing the sequencing experiment. The Bioimaging Platform of the LCSB is acknowledged for the support with the imaging analysis of the cell-based experiments. Meike Kasten, MD and Eva-Juliane Vollstedt, MD from the Institute of Neurogenetics, University of Luebeck are acknowledged for their contributions to the design and development of the LIPAD study. Prof. Dr. Özgür Öztop Çakmak and Prof. Dr. Ayşe Nazlı Başak from the Department of Neurology, Koc University, Turkey, are acknowledged for their contributions towards the Turkish LRRK2 samples. We thank Dr. Leonid Zaslavsky, Dr. Evan Bolton, and Dr. Tiejun Cheng from the PubChem Team for the help preparing the LRRK2 suspect list of chemicals. Dr. Gianfranco Frigerio is acknowledged for his inputs during the dust sample preparation and data processing. We acknowledge Veronica Codoni for her assistance with the power analysis calculation and its interpretation. The computational analyses presented in this paper were carried out using the HPC facilities at the University of Luxembourg [87], [139].

Funding

BTA is part of the "Microbiomes in One Health" PhD training program, which is supported by the PRIDE doctoral research funding scheme (PRIDE/11823097) of the Luxembourg National Research Fund (FNR). ELS acknowledges funding support from the Luxembourg National Research Fund (FNR) for project A18/BM/12341006. AG received funds from the FNR within the framework of the INTER grants "ProtectMove I and II" (FNR11250962 and INTER/DFG/19/14429377) and the ATTRACT career development grant "Model-IPD" (FNR9631103). The LIPAD study has been supported by institutional funds (Institute of Neurogenetics, University of Lübeck), and was partly supported by Centogene GmbH. Moreover, this study was supported by the German Research Foundation (DFG, ProtectMove FOR2488 to CK, NB, and AG).

References

[1] J. D. Steinmetz *et al.*, "Global, regional, and national burden of disorders affecting the nervous system, 1990–2021: a systematic analysis for the Global Burden of Disease Study 2021," *Lancet Neurol.*, vol. 23, no. 4, pp. 344–381, Apr. 2024, doi: 10.1016/S1474-4422(24)00038-3.

[2] S.-J. Chen and C.-H. Lin, "Gut microenvironmental changes as a potential trigger in Parkinson's disease through the gut–brain axis," *J. Biomed. Sci.*, vol. 29, no. 1, p. 54, Dec. 2022, doi: 10.1186/s12929-022-00839-6.

[3] S. Vascellari *et al.*, "Gut Microbiota and Metabolome Alterations Associated with Parkinson's Disease," *mSystems*, vol. 5, no. 5, pp. e00561-20, Oct. 2020, doi: 10.1128/mSystems.00561-20.

[4] B. Talavera Andújar *et al.*, "Studying the Parkinson's disease metabolome and exposome in biological samples through different analytical and cheminformatics approaches: a pilot study," *Anal. Bioanal. Chem.*, Jul. 2022, doi: 10.1007/s00216-022-04207-z.

[5] M. Lubomski, A. H. Tan, S.-Y. Lim, A. J. Holmes, R. L. Davis, and C. M. Sue, "Parkinson's disease and the gastrointestinal microbiome," *J. Neurol.*, vol. 267, no. 9, pp. 2507–2523, Sep. 2020, doi: 10.1007/s00415-019-09320-1.

[6] B. R. Bloem, M. S. Okun, and C. Klein, "Parkinson's disease," *The Lancet*, vol. 397, no. 10291, pp. 2284–2303, Jun. 2021, doi: 10.1016/S0140-6736(21)00218-X.

[7] S. Romano, G. M. Savva, J. R. Bedarf, I. G. Charles, F. Hildebrand, and A. Narbad, "Meta-analysis of the Parkinson's disease gut microbiome suggests alterations linked to intestinal inflammation," *Npj Park. Dis.*, vol. 7, no. 1, p. 27, Mar. 2021, doi: 10.1038/s41531-021-00156-z.

[8] A. Siderowf *et al.*, "Assessment of heterogeneity among participants in the Parkinson's Progression Markers Initiative cohort using α-synuclein seed amplification: a cross-sectional study," *Lancet Neurol.*, vol. 22, no. 5, pp. 407–417, May 2023, doi: 10.1016/S1474-4422(23)00109-6.

[9] S. A. Schneider and R. N. Alcalay, "Neuropathology of genetic synucleinopathies with parkinsonism: Review of the literature," *Mov. Disord.*, vol. 32, no. 11, pp. 1504–1523, Nov. 2017, doi: 10.1002/mds.27193.

[10] G. U. Höglinger *et al.*, "A biological classification of Parkinson's disease: the SynNeurGe research diagnostic criteria," *Lancet Neurol.*, vol. 23, no. 2, pp. 191–204, Feb. 2024, doi: 10.1016/S1474-4422(23)00404-0.

[11] S.-Y. Lim and C. Klein, "Parkinson's Disease is Predominantly a Genetic Disease," *J. Park. Dis.*, vol. 14, no. 3, pp. 467–482, Jan. 2024, doi: 10.3233/JPD-230376.

[12] S. R. Subramaniam and M.-F. Chesselet, "Mitochondrial dysfunction and oxidative stress in Parkinson's disease," *Prog. Neurobiol.*, vol. 106–107, pp. 17–32, Jul. 2013, doi: 10.1016/j.pneurobio.2013.04.004.

[13] A. Bose and M. F. Beal, "Mitochondrial dysfunction in Parkinson's disease," *J. Neurochem.*, vol. 139, no. S1, pp. 216–231, Oct. 2016, doi: 10.1111/jnc.13731.

[14] G. Bjørklund, M. Dadar, S. Chirumbolo, and J. Aaseth, "The Role of Xenobiotics and Trace Metals in Parkinson's Disease," *Mol. Neurobiol.*, vol. 57, no. 3, pp. 1405–1417, Mar. 2020, doi: 10.1007/s12035-019-01832-1.

[15] J. Trinh, E. L. Schymanski, S. Smajic, M. Kasten, E. Sammler, and A. Grünewald, "Molecular mechanisms defining penetrance of LRRK2-associated Parkinson's disease," *Med. Genet.*, vol. 34, no. 2, pp. 103–116, Jun. 2022, doi: 10.1515/medgen-2022-2127.

[16] V. Skrahina *et al.*, "The Rostock International Parkinson's Disease (ROPAD) Study: Protocol and Initial Findings," *Mov. Disord. Off. J. Mov. Disord. Soc.*, vol. 36, no. 4, pp. 1005–1010, Apr. 2021, doi: 10.1002/mds.28416.

[17] M. Miller, L. Cook, J. Verbrugge, P. D. Hodges, K. J. Head, and M. A. Nance, "Delivering Genetic Test Results for Parkinson Disease," *Neurol. Clin. Pract.*, vol. 14, no. 2, p. e200282, Apr. 2024, doi: 10.1212/CPJ.0000000000200282.

[18] G. Tsafaras and V. Baekelandt, "The role of LRRK2 in the periphery: link with Parkinson's disease and inflammatory diseases," *Neurobiol. Dis.*, vol. 172, p. 105806, Oct. 2022, doi: 10.1016/j.nbd.2022.105806.

[19] T. Usnich *et al.*, "LIPAD (LRRK2/Luebeck International Parkinson's Disease) Study Protocol: Deep Phenotyping of an International Genetic Cohort," *Front. Neurol.*, vol. 12, 2021, Accessed: Dec. 08, 2023. [Online]. Available: https://www.frontiersin.org/articles/10.3389/fneur.2021.710572

[20] D. G. Healy *et al.*, "Phenotype, genotype, and worldwide genetic penetrance of *LRRK2*-associated Parkinson's disease: a case-control study," *Lancet Neurol.*, vol. 7, no. 7, pp. 583–590, Jul. 2008, doi: 10.1016/S1474-4422(08)70117-0.

[21] F. Hentati, J. Trinh, C. Thompson, E. Nosova, M. J. Farrer, and J. O. Aasly, "LRRK2 parkinsonism in Tunisia and Norway: A comparative analysis of disease penetrance," *Neurology*, vol. 83, no. 6, pp. 568–569, Aug. 2014, doi: 10.1212/WNL.0000000000000675.

[22] S. A. Sakowski, E. J. Koubek, K. S. Chen, S. A. Goutman, and E. L. Feldman, "Role of the Exposome in Neurodegenerative Disease: Recent Insights and Future Directions," *Ann. Neurol.*, vol. 95, no. 4, pp. 635–652, 2024, doi: 10.1002/ana.26897.

[23] T. Lüth *et al.*, "Interaction of Mitochondrial Polygenic Score and Lifestyle Factors in LRRK2 p.Gly2019Ser Parkinsonism," *Mov. Disord. Off. J. Mov. Disord. Soc.*, vol. 38, no. 10, pp. 1837–1849, Oct. 2023, doi: 10.1002/mds.29563.

[24] Y. Shan, W. Wu, W. Fan, T. Haahtela, and G. Zhang, "House dust microbiome and human health risks," *Int. Microbiol.*, vol. 22, no. 3, pp. 297–304, Sep. 2019, doi: 10.1007/s10123-019-00057-5.

[25] L. Zhu, P. Fauser, L. Mikkelsen, H. Sanderson, and K. Vorkamp, "Suspect and non-target screening of semi-volatile emerging contaminants in indoor dust from Danish kindergartens," *Chemosphere*, vol. 345, p. 140451, Dec. 2023, doi: 10.1016/j.chemosphere.2023.140451.

[26] P. Rostkowski *et al.*, "The strength in numbers: comprehensive characterization of house dust using complementary mass spectrometric techniques," *Anal. Bioanal. Chem.*, vol. 411, no. 10, pp. 1957–1977, Apr. 2019, doi: 10.1007/s00216-019-01615-6.

[27] R. P. Schwarzenbach *et al.*, "The Challenge of Micropollutants in Aquatic Systems," *Science*, vol. 313, no. 5790, pp. 1072–1077, Aug. 2006, doi: 10.1126/science.1127291.
[28] C. Moschet, T. Anumol, B. M. Lew, D. H. Bennett, and T. M. Young, "Household dust as a repository of chemical accumulation: New insights from a comprehensive high-resolution mass spectrometry study," *Environ. Sci. Technol.*, vol. 52, no. 5, pp. 2878–2887, Mar. 2018, doi: 10.1021/acs.est.7b05767.
[29] S. Kim *et al.*, "PubChem 2023 update," *Nucleic Acids Res.*, vol. 51, no. D1, pp. D1373–D1380, Jan. 2023, doi: 10.1093/nar/gkac956.
[30] "PubChem Classification Browser." Accessed: May 19, 2024. [Online]. Available: https://pubchem.ncbi.nlm.nih.gov/classification/#hid=72
[31] E. Bolton, E. Schymanski, T. Kondic, P. Thiessen, and J. (Jeff) Zhang, "PubChemLite for Exposomics." Zenodo, Jun. 28, 2024. doi: 10.5281/ZENODO.12578095.
[32] E. L. Schymanski, T. Kondić, S. Neumann, P. A. Thiessen, J. Zhang, and E. E. Bolton, "Empowering large chemical knowledge bases for exposomics: PubChemLite meets MetFrag," *J. Cheminformatics*, vol. 13, no. 1, p. 19, Dec. 2021, doi: 10.1186/s13321-021-00489-0.
[33] H. Mohammed Taha *et al.*, "The NORMAN Suspect List Exchange (NORMAN-SLE): facilitating European and worldwide collaboration on suspect screening in high resolution mass spectrometry," *Environ. Sci. Eur.*, vol. 34, no. 1, p. 104, Oct. 2022, doi: 10.1186/s12302-022-00680-6.
[34] "NORMAN Network | NORMAN." Accessed: Mar. 07, 2024. [Online]. Available: https://www.norman-network.com/?q=node/4
[35] V. Dulio *et al.*, "The NORMAN Association and the European Partnership for Chemicals Risk Assessment (PARC): let's cooperate!," *Environ. Sci. Eur.*, vol. 32, no. 1, p. 100, Jul. 2020, doi: 10.1186/s12302-020-00375-w.
[36] P. von der Ohe and R. Aalizadeh, "S13 | EUCOSMETICS | Combined Inventory of Ingredients Employed in Cosmetic Products (2000) and Revised Inventory (2006)." Zenodo, May 28, 2020. doi: 10.5281/zenodo.3959386.
[37] N. Alygizakis and J. Slobodnik, "S32 | REACH2017 | >68,600 REACH Chemicals." Zenodo, Sep. 20, 2018. doi: 10.5281/zenodo.2653021.
[38] N. Baker, E. Schymanski, and A. Williams, "S37 | LITMINEDNEURO | Neurotoxicants from literature mining PubMed." Zenodo, Jun. 10, 2019. doi: 10.5281/zenodo.3242298.
[39] P. Haglund and P. Rostkowski, "S35 | INDOORCT16 | Indoor Environment Substances from 2016 Collaborative Trial," Feb. 2019, doi: 10.5281/zenodo.6848859.
[40] Y. Sun *et al.*, "Indoor microbiome, microbial and plant metabolites, chemical compounds, and asthma symptoms in junior high school students: a multicentre association study in Malaysia," *Eur. Respir. J.*, vol. 60, no. 5, p. 2200260, Nov. 2022, doi: 10.1183/13993003.00260-2022.
[41] Y. Sun *et al.*, "Indoor metabolites and chemicals outperform microbiome in classifying childhood asthma and allergic rhinitis," *Eco-Environ. Health*, vol. 2, no. 4, pp. 208–218, Dec. 2023, doi: 10.1016/j.eehl.2023.08.001.
[42] K. J. Locey and J. T. Lennon, "Scaling laws predict global microbial diversity," *Proc. Natl. Acad. Sci.*, vol. 113, no. 21, pp. 5970–5975, May 2016, doi: 10.1073/pnas.1521291113.

[43] J. R. Thompson *et al.*, "Bacterial Diversity in House Dust: Characterization of a Core Indoor Microbiome," *Front. Environ. Sci.*, vol. 9, Nov. 2021, doi: 10.3389/fenvs.2021.754657.
[44] D. S.-Q. Ooi *et al.*, "Developmental Origins of Health and Disease: Impact of environmental dust exposure in modulating microbiome and its association with non-communicable diseases," *J. Dev. Orig. Health Dis.*, vol. 11, no. 6, pp. 545–556, Dec. 2020, doi: 10.1017/S2040174420000549.
[45] K. Kowal, E. Żebrowska, and A. Chabowski, "Altered Sphingolipid Metabolism Is Associated With Asthma Phenotype in House Dust Mite-Allergic Patients," *Allergy Asthma Immunol. Res.*, vol. 11, no. 3, pp. 330–342, Jan. 2019, doi: 10.4168/aair.2019.11.3.330.
[46] S. J. Edwards and B. V. Kjellerup, "Applications of biofilms in bioremediation and biotransformation of persistent organic pollutants, pharmaceuticals/personal care products, and heavy metals," *Appl. Microbiol. Biotechnol.*, vol. 97, no. 23, pp. 9909–9921, Dec. 2013, doi: 10.1007/s00253-013-5216-z.
[47] C. D. Kassotis, K. Hoffman, and H. M. Stapleton, "Characterization of Adipogenic Activity of House Dust Extracts and Semi-Volatile Indoor Contaminants in 3T3-L1 Cells," *Environ. Sci. Technol.*, vol. 51, no. 15, pp. 8735–8745, Aug. 2017, doi: 10.1021/acs.est.7b01788.
[48] L. Melymuk, H. Demirtepe, and S. R. Jílková, "Indoor dust and associated chemical exposures," *Curr. Opin. Environ. Sci. Health*, vol. 15, pp. 1–6, Jun. 2020, doi: 10.1016/j.coesh.2020.01.005.
[49] P. Li *et al.*, "Gut Microbiota Dysbiosis Is Associated with Elevated Bile Acids in Parkinson's Disease," *Metabolites*, vol. 11, no. 1, p. 29, Jan. 2021, doi: 10.3390/metabo11010029.
[50] S. F. Graham *et al.*, "Metabolomic Profiling of Bile Acids in an Experimental Model of Prodromal Parkinson's Disease," *Metabolites*, vol. 8, no. 4, p. 71, Oct. 2018, doi: 10.3390/metabo8040071.
[51] J. S. Loh *et al.*, "Microbiota–gut–brain axis and its therapeutic applications in neurodegenerative diseases," *Signal Transduct. Target. Ther.*, vol. 9, no. 1, pp. 1–53, Feb. 2024, doi: 10.1038/s41392-024-01743-1.
[52] A. Westenberger *et al.*, "Relevance of genetic testing in the gene-targeted trial era: the Rostock Parkinson's disease study," *Brain*, vol. 147, no. 8, pp. 2652–2667, Aug. 2024, doi: 10.1093/brain/awae188.
[53] F. Dubocq, A. Kärrman, J. Gustavsson, and T. Wang, "Comprehensive chemical characterization of indoor dust by target, suspect screening and nontarget analysis using LC-HRMS and GC-HRMS," *Environ. Pollut.*, vol. 276, p. 116701, May 2021, doi: 10.1016/j.envpol.2021.116701.
[54] D. Broadhurst *et al.*, "Guidelines and considerations for the use of system suitability and quality control samples in mass spectrometry assays applied in untargeted clinical metabolomic studies," *Metabolomics*, vol. 14, no. 6, p. 72, May 2018, doi: 10.1007/s11306-018-1367-3.
[55] "DNeasy PowerLyzer PowerSoil Kit." Accessed: Mar. 13, 2024. [Online]. Available: https://www.qiagen.com/us/products/discovery-and-translational-research/dna-rna-purification/dna-purification/microbial-dna/dneasy-powerlyzer-powersoil-kit

[56] T. Cajka, J. T. Smilowitz, and O. Fiehn, "Validating Quantitative Untargeted Lipidomics Across Nine Liquid Chromatography–High-Resolution Mass Spectrometry Platforms," *Anal. Chem.*, vol. 89, no. 22, pp. 12360–12368, Nov. 2017, doi: 10.1021/acs.analchem.7b03404.

[57] M. Lange and M. Fedorova, "Evaluation of lipid quantification accuracy using HILIC and RPLC MS on the example of NIST® SRM® 1950 metabolites in human plasma," *Anal. Bioanal. Chem.*, vol. 412, no. 15, pp. 3573–3584, Jun. 2020, doi: 10.1007/s00216-020-02576-x.

[58] M. C. Chambers *et al.*, "A cross-platform toolkit for mass spectrometry and proteomics," *Nat. Biotechnol.*, vol. 30, no. 10, pp. 918–920, Oct. 2012, doi: 10.1038/nbt.2377.

[59] R. Helmus, T. L. ter Laak, A. P. van Wezel, P. de Voogt, and E. L. Schymanski, *patRoon: open source software platform for environmental mass spectrometry based non-target screening*. (Jan. 2021). R. doi: 10.1186/s13321-020-00477-w.

[60] R. Helmus, B. van de Velde, A. M. Brunner, T. L. ter Laak, A. P. van Wezel, and E. L. Schymanski, "patRoon 2.0: Improved non-target analysis workflows including automated transformation product screening," *J. Open Source Softw.*, vol. 7, no. 71, p. 4029, Mar. 2022, doi: 10.21105/joss.04029.

[61] H. Tsugawa *et al.*, "MS-DIAL: data-independent MS/MS deconvolution for comprehensive metabolome analysis," *Nat. Methods*, vol. 12, no. 6, Art. no. 6, Jun. 2015, doi: 10.1038/nmeth.3393.

[62] Begoña Talavera Andújar, "uniluxembourg / LCSB / Environmental Cheminformatics / PD-LRRK2 · GitLab," GitLab. Accessed: Jul. 18, 2024. [Online]. Available: https://gitlab.com/uniluxembourg/lcsb/eci/pd-lrrk2

[63] T. Kind, K.-H. Liu, D. Y. Lee, B. DeFelice, J. K. Meissen, and O. Fiehn, "LipidBlast in silico tandem mass spectrometry database for lipid identification," *Nat. Methods*, vol. 10, no. 8, Art. no. 8, Aug. 2013, doi: 10.1038/nmeth.2551.

[64] J. P. Koelmel *et al.*, "LipidMatch: an automated workflow for rule-based lipid identification using untargeted high-resolution tandem mass spectrometry data," *BMC Bioinformatics*, vol. 18, no. 1, p. 331, Jul. 2017, doi: 10.1186/s12859-017-1744-3.

[65] N. Dodder and K. Mullen, *OrgMassSpecR: Organic Mass Spectrometry*. (Aug. 13, 2017). Accessed: Jan. 29, 2024. [Online]. Available: https://cran.r-project.org/web/packages/OrgMassSpecR/index.html

[66] "Nontargeted Comprehensive Two-Dimensional Gas Chromatography/Time-of-Flight Mass Spectrometry Method and Software for Inventorying Persistent and Bioaccumulative Contaminants in Marine Environments | Environmental Science & Technology." Accessed: Jan. 29, 2024. [Online]. Available: https://pubs.acs.org/doi/10.1021/es301139q

[67] G. Yu, C. Xu, D. Zhang, F. Ju, and Y. Ni, "MetOrigin: Discriminating the origins of microbial metabolites for integrative analysis of the gut microbiome and metabolome," *iMeta*, vol. 1, no. 1, p. e10, 2022, doi: 10.1002/imt2.10.

[68] "PubChem Classification Browser." Accessed: May 20, 2024. [Online]. Available: https://pubchem.ncbi.nlm.nih.gov/classification/#hid=101

[69] J. Mayfield, "CDK Depict Web Interface." 2023. Accessed: Mar. 09, 2023. [Online]. Available: https://www.simolecule.com/cdkdepict/depict.html

[70] Z. Pang *et al.*, "MetaboAnalyst 6.0: towards a unified platform for metabolomics data processing, analysis and interpretation," *Nucleic Acids Res.*, p. gkae253, Apr. 2024, doi: 10.1093/nar/gkae253.
[71] "LIPEA | What is LIPEA?" Accessed: Mar. 05, 2024. [Online]. Available: https://hyperlipea.org/about/what
[72] S. Narayanasamy *et al.*, "IMP: a pipeline for reproducible reference-independent integrated metagenomic and metatranscriptomic analyses," *Genome Biol.*, vol. 17, no. 1, p. 260, Dec. 2016, doi: 10.1186/s13059-016-1116-8.
[73] Shaman Narayanasamy, Yohan Jarosz, and Anna Heintz-Buschart, "IMP / IMP3 · GitLab," GitLab. Accessed: Mar. 26, 2024. [Online]. Available: https://gitlab.lcsb.uni.lu/IMP/imp3
[74] T. Seemann, "Prokka: rapid prokaryotic genome annotation," *Bioinformatics*, vol. 30, no. 14, pp. 2068–2069, Jul. 2014, doi: 10.1093/bioinformatics/btu153.
[75] J. Chong, P. Liu, G. Zhou, and J. Xia, "Using MicrobiomeAnalyst for comprehensive statistical, functional, and meta-analysis of microbiome data," *Nat. Protoc.*, vol. 15, no. 3, pp. 799–821, Mar. 2020, doi: 10.1038/s41596-019-0264-1.
[76] Y. Lu, G. Zhou, J. Ewald, Z. Pang, T. Shiri, and J. Xia, "MicrobiomeAnalyst 2.0: comprehensive statistical, functional and integrative analysis of microbiome data," *Nucleic Acids Res.*, vol. 51, no. W1, pp. W310–W318, Jul. 2023, doi: 10.1093/nar/gkad407.
[77] K. S. Andersen, *KasperSkytte/ampvis2*. (Jan. 16, 2024). R. Accessed: Feb. 19, 2024. [Online]. Available: https://github.com/KasperSkytte/ampvis2
[78] "KEGGREST," Bioconductor. Accessed: Mar. 12, 2024. [Online]. Available: http://bioconductor.org/packages/KEGGREST/
[79] F. Rohart, B. Gautier, A. Singh, and K.-A. L. Cao, "mixOmics: An R package for 'omics feature selection and multiple data integration," *PLOS Comput. Biol.*, vol. 13, no. 11, p. e1005752, Nov. 2017, doi: 10.1371/journal.pcbi.1005752.
[80] *ConesaLab/MultiPower*. (Mar. 12, 2024). R. ConesaLab - Genomics of gene expression. Accessed: Mar. 27, 2024. [Online]. Available: https://github.com/ConesaLab/MultiPower
[81] S. Tarazona *et al.*, "Harmonization of quality metrics and power calculation in multi-omic studies," *Nat. Commun.*, vol. 11, no. 1, p. 3092, Jun. 2020, doi: 10.1038/s41467-020-16937-8.
[82] X. Qing, J. Walter, J. Jarazo, J. Arias-Fuenzalida, A.-L. Hillje, and J. C. Schwamborn, "CRISPR/Cas9 and piggyBac-mediated footprint-free LRRK2-G2019S knock-in reveals neuronal complexity phenotypes and α-Synuclein modulation in dopaminergic neurons," *Stem Cell Res.*, vol. 24, pp. 44–50, Oct. 2017, doi: 10.1016/j.scr.2017.08.013.
[83] P. Reinhardt *et al.*, "Genetic Correction of a LRRK2 Mutation in Human iPSCs Links Parkinsonian Neurodegeneration to ERK-Dependent Changes in Gene Expression," *Cell Stem Cell*, vol. 12, no. 3, pp. 354–367, Mar. 2013, doi: 10.1016/j.stem.2013.01.008.
[84] S. L. Nickels *et al.*, "Impaired serine metabolism complements LRRK2-G2019S pathogenicity in PD patients," *Parkinsonism Relat. Disord.*, vol. 67, pp. 48–55, Oct. 2019, doi: 10.1016/j.parkreldis.2019.09.018.

[85] P. Reinhardt *et al.*, "Derivation and Expansion Using Only Small Molecules of Human Neural Progenitors for Neurodegenerative Disease Modeling," *PLOS ONE*, vol. 8, no. 3, p. e59252, Mar. 2013, doi: 10.1371/journal.pone.0059252.

[86] A. S. Baumuratov *et al.*, "Enteric neurons from Parkinson's disease patients display ex vivo aberrations in mitochondrial structure," *Sci. Rep.*, vol. 6, no. 1, p. 33117, Sep. 2016, doi: 10.1038/srep33117.

[87] "Homepage | HPC @ Uni.lu." Accessed: Mar. 26, 2024. [Online]. Available: https://hpc.uni.lu/

[88] W. Lilienblum *et al.*, "Alternative methods to safety studies in experimental animals: role in the risk assessment of chemicals under the new European Chemicals Legislation (REACH)," *Arch. Toxicol.*, vol. 82, no. 4, pp. 211–236, Apr. 2008, doi: 10.1007/s00204-008-0279-9.

[89] S. Salis *et al.*, "Occurrence of imidacloprid, carbendazim, and other biocides in Italian house dust: Potential relevance for intakes in children and pets," *J. Environ. Sci. Health Part B*, vol. 52, no. 9, pp. 699–709, Sep. 2017, doi: 10.1080/03601234.2017.1331675.

[90] K. Groh and E. Schymanski, "S49 | CPPDBLISTB | Database of Chemicals possibly (List B) associated with Plastic Packaging (CPPdb)." Zenodo, Mar. 06, 2019. doi: 10.5281/ZENODO.2658152.

[91] M. Naderi and R. W. M. Kwong, "A comprehensive review of the neurobehavioral effects of bisphenol S and the mechanisms of action: New insights from in vitro and in vivo models," *Environ. Int.*, vol. 145, p. 106078, Dec. 2020, doi: 10.1016/j.envint.2020.106078.

[92] C. Hu, Z. Huang, B. Sun, M. Liu, L. Tang, and L. Chen, "Metabolomic profiles in zebrafish larvae following probiotic and perfluorobutanesulfonate coexposure," *Environ. Res.*, vol. 204, p. 112380, Mar. 2022, doi: 10.1016/j.envres.2021.112380.

[93] E. Gyimah *et al.*, "Developmental neurotoxicity of low concentrations of bisphenol A and S exposure in zebrafish," *Chemosphere*, vol. 262, p. 128045, Jan. 2021, doi: 10.1016/j.chemosphere.2020.128045.

[94] H. An, H. Yu, Y. Wei, F. Liu, and J. Ye, "Disrupted metabolic pathways and potential human diseases induced by bisphenol S," *Environ. Toxicol. Pharmacol.*, vol. 88, p. 103751, Nov. 2021, doi: 10.1016/j.etap.2021.103751.

[95] E. Schirmer, S. Schuster, and P. Machnik, "Bisphenols exert detrimental effects on neuronal signaling in mature vertebrate brains," *Commun. Biol.*, vol. 4, no. 1, pp. 1–9, Apr. 2021, doi: 10.1038/s42003-021-01966-w.

[96] I. T. Cousins *et al.*, "The high persistence of PFAS is sufficient for their management as a chemical class," *Environ. Sci. Process. Impacts*, vol. 22, no. 12, pp. 2307–2312, 2020, doi: 10.1039/D0EM00355G.

[97] E. K. Min *et al.*, "Integrative multi-omics reveals analogous developmental neurotoxicity mechanisms between perfluorobutanesulfonic acid and perfluorooctanesulfonic acid in zebrafish," *J. Hazard. Mater.*, vol. 457, p. 131714, Sep. 2023, doi: 10.1016/j.jhazmat.2023.131714.

[98] D. van der Merwe, A. Jordaan, and M. van den Berg, "Case report: fipronil contamination of chickens in the Netherlands and surrounding countries," in *Chemical hazards in foods of animal origin*, Wageningen Academic, 2019, pp. 567–584. doi: 10.3920/978-90-8686-877-3_23.

[99] J. Kathage, P. Castañera, J. L. Alonso-Prados, M. Gómez-Barbero, and E. Rodríguez-Cerezo, "The impact of restrictions on neonicotinoid and fipronil insecticides on pest management in maize, oilseed rape and sunflower in eight European Union regions," *Pest Manag. Sci.*, vol. 74, no. 1, pp. 88–99, 2018, doi: 10.1002/ps.4715.

[100] C. Testa, S. Salis, N. Rubattu, P. Roncada, R. Miniero, and G. Brambilla, "Occurrence of Fipronil in residential house dust in the presence and absence of pets: a hint for a comprehensive toxicological assessment," *J. Environ. Sci. Health Part B*, vol. 54, no. 6, pp. 441–448, Jun. 2019, doi: 10.1080/03601234.2019.1607133.

[101] H. De Wever, H. Verachtert, and P. Besse, "Microbial transformations of 2-substituted benzothiazoles," *Appl. Microbiol. Biotechnol.*, vol. 57, no. 5–6, pp. 620–625, Dec. 2001, doi: 10.1007/s00253-001-0842-2.

[102] C. Liao, U.-J. Kim, and K. Kannan, "A Review of Environmental Occurrence, Fate, Exposure, and Toxicity of Benzothiazoles," *Environ. Sci. Technol.*, vol. 52, no. 9, pp. 5007–5026, May 2018, doi: 10.1021/acs.est.7b05493.

[103] J. Gu, L. Guo, C. Chen, G. Ji, and L. Wang, "Neurobehavioral toxic effects and mechanisms of 2-aminobenzothiazole exposure on zebrafish," *Sci. Total Environ.*, vol. 913, p. 169495, Feb. 2024, doi: 10.1016/j.scitotenv.2023.169495.

[104] M. W. Hornung *et al.*, "*In Vitro* , *Ex Vivo* , and *In Vivo* Determination of Thyroid Hormone Modulating Activity of Benzothiazoles," *Toxicol. Sci.*, vol. 146, no. 2, pp. 254–264, Aug. 2015, doi: 10.1093/toxsci/kfv090.

[105] S. Cao *et al.*, "Prenatal exposure to benzotriazoles and benzothiazoles and child neurodevelopment: A longitudinal study," *Sci. Total Environ.*, vol. 865, p. 161188, Mar. 2023, doi: 10.1016/j.scitotenv.2022.161188.

[106] N. J. Nielsen, P. Christensen, K. G. Poulsen, and J. H. Christensen, "Investigation of micropollutants in household waste fractions processed by anaerobic digestion: target analysis, suspect- and non-target screening," *Environ. Sci. Pollut. Res.*, vol. 30, no. 16, pp. 48491–48507, Feb. 2023, doi: 10.1007/s11356-023-25692-4.

[107] L. Palacios Colón, A. J. Rascón, L. Hejji, A. Azzouz, and E. Ballesteros, "Validation and Use of an Accurate, Sensitive Method for Sample Preparation and Gas Chromatography–Mass Spectrometry Determination of Different Endocrine-Disrupting Chemicals in Dairy Products," *Foods*, vol. 10, no. 5, p. 1040, May 2021, doi: 10.3390/foods10051040.

[108] S. Andres and V. Dulio, "S109 | PARCEDC | List of 7074 potential endocrine disrupting compounds (EDCs) by PARC T4.2." Zenodo, Apr. 08, 2024. doi: 10.5281/zenodo.10944199.

[109] N. Nazar *et al.*, "Untargeted metabolomics reveals potential health risks associated with chronic exposure to environmentally relevant concentrations of 2-Phenylphenol," *Sci. Total Environ.*, vol. 912, p. 169172, Feb. 2024, doi: 10.1016/j.scitotenv.2023.169172.

[110] Y. Shan *et al.*, "Modern urbanization has reshaped the bacterial microbiome profiles of house dust in domestic environments," *World Allergy Organ. J.*, vol. 13, no. 8, p. 100452, Aug. 2020, doi: 10.1016/j.waojou.2020.100452.

[111] J. R. Thompson *et al.*, "Bacterial Diversity in House Dust: Characterization of a Core Indoor Microbiome," *Front. Environ. Sci.*, vol. 9, 2021, Accessed: Mar. 01, 2024. [Online]. Available: https://www.frontiersin.org/articles/10.3389/fenvs.2021.754657

[112] J. C. Boktor *et al.*, "Integrated Multi-Cohort Analysis of the Parkinson's Disease Gut Metagenome," *Mov. Disord.*, vol. 38, no. 3, pp. 399–409, 2023, doi: 10.1002/mds.29300.

[113] R. Eichenlaub and K.-H. Gartemann, "The Clavibacter michiganensis Subspecies: Molecular Investigation of Gram-Positive Bacterial Plant Pathogens," *Annu. Rev. Phytopathol.*, vol. 49, no. 1, pp. 445–464, 2011, doi: 10.1146/annurev-phyto-072910-095258.

[114] P. A. B. Pereira, V. T. E. Aho, L. Paulin, E. Pekkonen, P. Auvinen, and F. Scheperjans, "Oral and nasal microbiota in Parkinson's disease," *Parkinsonism Relat. Disord.*, vol. 38, pp. 61–67, May 2017, doi: 10.1016/j.parkreldis.2017.02.026.

[115] Y. Ma *et al.*, "Nocardioides: 'Specialists' for Hard-to-Degrade Pollutants in the Environment," *Molecules*, vol. 28, no. 21, Art. no. 21, Jan. 2023, doi: 10.3390/molecules28217433.

[116] Y. Qian *et al.*, "Alteration of the fecal microbiota in Chinese patients with Parkinson's disease," *Brain. Behav. Immun.*, vol. 70, pp. 194–202, May 2018, doi: 10.1016/j.bbi.2018.02.016.

[117] R. G. Kleespies, B. A. Federici, and A. Leclerque, "Ultrastructural characterization and multilocus sequence analysis (MLSA) of '*Candidatus* Rickettsiella isopodorum', a new lineage of intracellular bacteria infecting woodlice (Crustacea: Isopoda)," *Syst. Appl. Microbiol.*, vol. 37, no. 5, pp. 351–359, Jul. 2014, doi: 10.1016/j.syapm.2014.04.001.

[118] H. Takeshige-Amano *et al.*, "Shared Metabolic Profile of Caffeine in Parkinsonian Disorders," *Mov. Disord.*, vol. 35, no. 8, pp. 1438–1447, Aug. 2020, doi: 10.1002/mds.28068.

[119] M. Fujimaki *et al.*, "Serum caffeine and metabolites are reliable biomarkers of early Parkinson disease," *Neurology*, vol. 90, no. 5, Jan. 2018, doi: 10.1212/WNL.0000000000004888.

[120] C. Gonzalez-Riano *et al.*, "Prognostic biomarkers of Parkinson's disease in the Spanish EPIC cohort: a multiplatform metabolomics approach," *Npj Park. Dis.*, vol. 7, no. 1, pp. 1–12, Aug. 2021, doi: 10.1038/s41531-021-00216-4.

[121] Y. Matsuda, K. Higashino, K. Adachi, Y. Amuro, and T. Hada, "Production of pipecolic acid from intestinal bacteria: Plasma levels of pipecolic acid in patients with liver cirrhosis decreased after oral kanamycin administration," *Int. Hepatol. Commun.*, vol. 4, no. 1, pp. 26–34, Jul. 1995, doi: 10.1016/0928-4346(95)00210-A.

[122] G. R. Dalazen *et al.*, "Pipecolic acid induces oxidative stress in vitro in cerebral cortex of young rats and the protective role of lipoic acid," *Metab. Brain Dis.*, vol. 29, no. 1, pp. 175–183, Mar. 2014, doi: 10.1007/s11011-013-9466-3.

[123] T.-K. Lin *et al.*, "When Friendship Turns Sour: Effective Communication Between Mitochondria and Intracellular Organelles in Parkinson's Disease," *Front. Cell Dev. Biol.*, vol. 8, p. 607392, Nov. 2020, doi: 10.3389/fcell.2020.607392.

[124] J. Galper *et al.*, "Lipid pathway dysfunction is prevalent in patients with Parkinson's disease," *Brain J. Neurol.*, p. awac176, May 2022, doi: 10.1093/brain/awac176.

[125] L. A. Dahabiyeh, R. M. Nimer, M. Rashed, J. D. Wells, and O. Fiehn, "Serum-Based Lipid Panels for Diagnosis of Idiopathic Parkinson's Disease," *Metabolites*, vol. 13, no. 9, Art. no. 9, Sep. 2023, doi: 10.3390/metabo13090990.

[126] J. Fernández-Irigoyen, P. Cartas-Cejudo, M. Iruarrizaga-Lejarreta, and E. Santamaría, "Alteration in the Cerebrospinal Fluid Lipidome in Parkinson's Disease: A Post-Mortem Pilot Study," *Biomedicines*, vol. 9, no. 5, Art. no. 5, May 2021, doi: 10.3390/biomedicines9050491.

[127] K.-H. Chang, M.-L. Cheng, H.-Y. Tang, C.-Y. Huang, H.-C. Wu, and C.-M. Chen, "Alterations of Sphingolipid and Phospholipid Pathways and Ornithine Level in the Plasma as Biomarkers of Parkinson's Disease," *Cells*, vol. 11, no. 3, Art. no. 3, Jan. 2022, doi: 10.3390/cells11030395.

[128] J. Zeng *et al.*, "Lipidome disturbances in preadipocyte differentiation associated with bisphenol A and replacement bisphenol S exposure," *Sci. Total Environ.*, vol. 753, p. 141949, Jan. 2021, doi: 10.1016/j.scitotenv.2020.141949.

[129] C. Zhao, Z. Tang, J. Yan, J. Fang, H. Wang, and Z. Cai, "Bisphenol S exposure modulate macrophage phenotype as defined by cytokines profiling, global metabolomics and lipidomics analysis," *Sci. Total Environ.*, vol. 592, pp. 357–365, Aug. 2017, doi: 10.1016/j.scitotenv.2017.03.035.

[130] B. Talavera Andújar *et al.*, "Can Small Molecules Provide Clues on Disease Progression in Cerebrospinal Fluid from Mild Cognitive Impairment and Alzheimer's Disease Patients?," *Environ. Sci. Technol.*, Feb. 2024, doi: 10.1021/acs.est.3c10490.

[131] I. Mohanty *et al.*, "The changing metabolic landscape of bile acids – keys to metabolism and immune regulation," *Nat. Rev. Gastroenterol. Hepatol.*, vol. 21, no. 7, pp. 493–516, Jul. 2024, doi: 10.1038/s41575-024-00914-3.

[132] Y. Xu *et al.*, "Effects and mechanisms of bisphenols exposure on neurodegenerative diseases risk: A systemic review," *Sci. Total Environ.*, vol. 919, p. 170670, Apr. 2024, doi: 10.1016/j.scitotenv.2024.170670.

[133] F. Singh, A. R. Prescott, P. Rosewell, G. Ball, A. D. Reith, and I. G. Ganley, "Pharmacological rescue of impaired mitophagy in Parkinson's disease-related LRRK2 G2019S knock-in mice," *eLife*, vol. 10, p. e67604, Aug. 2021, doi: 10.7554/eLife.67604.

[134] G. A. Lancaster, S. Dodd, and P. R. Williamson, "Design and analysis of pilot studies: recommendations for good practice," *J. Eval. Clin. Pract.*, vol. 10, no. 2, pp. 307–312, 2004, doi: 10.1111/j..2002.384.doc.x.

[135] R. L. Foster, "What a pilot study is and what it is not," *J. Spec. Pediatr. Nurs.*, vol. 18, no. 1, pp. 1–2, 2013, doi: 10.1111/jspn.12015.

[136] E. Fuentes-Ferragud, P. Miralles, A. López, M. Ibáñez, and C. Coscollà, "Non-target screening and human risk assessment for adult and child populations of semi-volatile organic compounds in residential indoor dust in Spain," *Chemosphere*, vol. 340, p. 139879, Nov. 2023, doi: 10.1016/j.chemosphere.2023.139879.

[137] B. J. Kunath, C. De Rudder, C. C. Laczny, E. Letellier, and P. Wilmes, "The oral–gut microbiome axis in health and disease," *Nat. Rev. Microbiol.*, pp. 1–15, Jul. 2024, doi: 10.1038/s41579-024-01075-5.

[138] A. David *et al.*, "Towards a comprehensive characterisation of the human internal chemical exposome: Challenges and perspectives," *Environ. Int.*, vol. 156, p. 106630, Nov. 2021, doi: 10.1016/j.envint.2021.106630.

[139] S. Varrette, P. Bouvry, H. Cartiaux, and F. Georgatos, "Management of an academic HPC cluster: The UL experience," in *2014 International Conference on High Performance Computing & Simulation (HPCS)*, Jul. 2014, pp. 959–967. doi: 10.1109/HPCSim.2014.6903792.